2.5 Department of Theory

Director:

Walter Thiel (born 1949)

Further group leaders:

Mario Barbatti (born 1971)
Left the Institute in 2015

Elsa Sánchez-García (born 1976)

Matthias Heyden (born 1981)

Michael Roemelt (born 1982)
Joined the Institute in 2015

Curriculum Vitae: Walter Thiel

1949	Born in Treysa, Germany
1966-1971	Chemistry studies at Universität Marburg
1971-1973	Doctoral studies at Universität Marburg, with A. Schweig
1973-1975	Postdoctoral fellow at the University of Texas at Austin, with M. J. S. Dewar
1975-1982	Research scientist at Universität Marburg
1981	Habilitation for Theoretical Chemistry
1983-1992	Associate Professor of Theoretical Chemistry at Universität Wuppertal
1987	Guest Professor at the University of California at Berkeley
1992-1999	Full Professor of Chemistry at Universität Zürich
1999	Director at the Max-Planck-Institut für Kohlenforschung in Mülheim/Ruhr
2001	Honorary Professor at Universität Düsseldorf

Awards and Honors

1969-1974	Studienstiftung des deutschen Volkes
1975-1977	Liebig Fellowship, Verband der Chemischen Industrie
1982	Heisenberg Fellowship, Deutsche Forschungsgemeinschaft
1988	Förderpreis, Alfried-Krupp Stiftung
1991	Member, European Academy of Sciences and Arts
2002	Schrödinger Medal, World Association of Theoretical Chemists
2007	Member, Deutsche Akademie der Naturforscher Leopoldina
2007	Member, International Academy of Quantum Molecular Sciences
2008	Member, Nordrhein-Westfälische Akademie der Wissenschaften
2009	Festschrift, Journal of Physical Chemistry A 2009, 113 (43), 11455-12044
2012	Liebig Medal, German Chemical Society
2014	ERC Advanced Grant, European Research Council
2014	Robert Bunsen Lecture, Deutsche Bunsengesellschaft

Special Activities

1986-1992	Member of the Board, Institut für Angewandte Informatik, Wuppertal
1990-1992	Speaker, DFG-Forschergruppe: Reaktive Moleküle
1997-2014	Advisory Editor, Theoretical Chemistry Accounts
1998-	Advisory Editor, Journal of Computational Chemistry
2000-2008	Reviewer (Fachkollegiat), Deutsche Forschungsgemeinschaft

2000-2006	Member of the Board (Lenkungsausschuss), Bavarian Supercomputer Center (Höchstleistungsrechenzentrum Bayern)
2001-2005	Chairman, Arbeitsgemeinschaft Theoretische Chemie
2002-2008	Section Editor, Encyclopedia of Computational Chemistry
2004-2007	Member, Ständiger Ausschuss der Bunsengesellschaft
2004-2017	Member of the Scientific Advisory Board, Lise Meitner Minerva Center for Quantum Chemistry, Jerusalem/Haifa, Israel
2006-2008	Managing Director, Max-Planck-Institut für Kohlenforschung
2006-2012	Chairman, BAR Committee of the Max Planck Society
2006-2013	Member of the Kuratorium, Angewandte Chemie
2008-	Associate Editor, WIRES: Computational Molecular Sciences
2009-	Member of the International Advisory Board, State Key Laboratory of Physical Chemistry (PCOSS), Xiamen, China
2010	Chairman, Gordon Conference on Computational Chemistry
2011-2014	Member of the International Advisory Board, Institute of Organic Chemistry and Biochemistry, Prague, Czech Republic
2011-2017	President, World Association of Theoretical and Computational Chemists
2012-2013	Editorial Advisory Board, ACS Catalysis
2012-2014	Editorial Advisory Board, Accounts of Chemical Research
2012-2015	Member of the Board of Governors, German Chemical Society
2013-	Member of the Scientific Advisory Board, Institute of Chemical Research of Catalonia, Tarragona, Spain
2015	Managing Director, Max-Planck-Institut für Kohlenforschung

Research in the Department of Theory

In the reporting period, the Department of Theory comprised the research group of Prof. Walter Thiel and up to four junior groups headed by PD Dr. Mario Barbatti, Dr. Elsa Sánchez-García, Dr. Matthias Heyden, and Dr. Michael Roemelt.

The central research objectives in the Department are theoretical developments to extend the scope of computational methodology, and applications to study problems of current chemical interest by computation. Such applications are mostly conducted in close cooperation with experimental partners.

In the group of Prof. Thiel, the main field of research is quantum chemistry. Methodological developments and chemical applications are considered to be of equal importance. The research interests range from accurate and almost quantitative calculations on small molecules to the approximate modeling of very large molecules. The activities of the group cover ab initio methods (e.g., coupled cluster approaches), density functional theory (DFT), semiempirical methods (orthogonalization models, OMx), and combined quantum mechanical/molecular mechanical methods (QM/MM). Applications in these four areas mainly focus on the vibration-rotation and electronic spectroscopy of small molecules, catalytic reactions of transition metal compounds, electronically excited states in large molecules, and reaction mechanisms in enzymes.

The group of Dr. Barbatti uses ab initio and density functional methods to study photoinduced processes in organic molecules. One major aim is to improve excited-state simulation methods by implementing new algorithms in the Newton-X code. Applications include nonadiabatic dynamics simulations of ultrafast excited-state relaxation processes in biologically relevant molecules and in photovoltaics.

The research in the group of Dr. Sánchez-García focuses on molecular interactions in organic and biological systems, on their relevance in the realm of chemical and biochemical reactivity, and on the development and application of multi-scale modeling approaches. Current research topics include protein-ligand and protein-protein interactions, computational mutagenesis, and solvent effects on reactivity.

The group of Dr. Heyden uses classical molecular dynamics methods to investigate biomolecular solvation phenomena. The group develops novel simulation and analysis procedures to study microscopic contributions to the solvation free energy, with a

partitioning into local enthalpy and entropy terms. Another aim is to improve implicit solvent simulations of concentrated biomolecular solutions on the meso-scale.

The group of Dr. Roemelt aims at the development of highly accurate ab initio quantum-chemical methods for complex molecular systems, with focus on the density matrix renormalization group (DMRG) approach. Targeted are extensions to the DMRG ansatz that improve its accuracy and allow the calculation of magnetic properties. DMRG applications address the properties of transition metal compounds.

Several cooperations between the Department of Theory and the experimental groups in the Institute have been established over the past years. There have been major collaborative projects on transition-metal catalysis (Fürstner, Alcarazo, Maulide, Klussmann), organocatalysis (List), and cellulose depolymerization (Schüth). Several groups of the Department (Thiel, Sánchez-García, Heyden) enjoy close cooperations with experimental partners in the RESOLV Cluster of Excellence on solvation science.

More detailed information on the research areas of the Department is available in the following eight individual reports and in the scientific papers published in 2014-2016. For the sake of brevity, some of these papers have not been discussed in the individual reports and should therefore be consulted directly, if necessary.

The tenure of the Director of the Department, Prof. Thiel, will end in March 2017. As an Emeritus, he will continue to do research in the framework of an ERC Advanced Grant (2014-2018), which targets the development of improved semiempirical methods with orthogonalization and dispersion corrections, as well as the application of these methods, for example, in excited-state dynamics simulations. Among the group leaders, Dr. Barbatti has left the Institute in 2015 to take up a professorship at the Université Aix-Marseille. Dr. Sánchez-García has been offered a professorship (W2) in computational biology at the University Duisburg-Essen (UDE) and is expected to move to UDE in early 2017. Dr. Heyden has been selected as junior group leader in a thematically open RESOLV competition and is hosted by our Institute during the term of his appointment (currently 2014-2017). In recognition of his outstanding Ph.D. thesis, Dr. Roemelt has been awarded the leadership of an Otto Hahn group by the Max Planck Society for the period 2015-2017.

The Institute has selected Prof. Frank Neese as next Director of the Department of Theory. Assuming a smooth appointment process, he can start in April 2017.

2.5.1 Research area "Ab initio methods" (W. Thiel)

Involved: A. Altun, J. Breidung, G. Cui, A. Nikiforov, A. Owens

Objective: Vibration-rotation and electronic spectra of small molecules are computed with high accuracy using high-level ab initio calculations with large basis sets. The vibration-rotation studies make use of a general variational treatment of nuclear motion previously developed in our group that allows the accurate prediction of rovibrational energies and intensities. Correlated ab initio methods are also applied for validation and benchmark purposes, especially in studies on electronically excited states.

Results: The theoretical prediction of vibration-rotation spectra requires the generation of accurate potential energy and dipole moment surfaces, followed by the variational calculation of rovibrational energies and intensities. For the former task, we employ ab initio electronic structure methods, typically coupled cluster theory with complete basis set extrapolation and corrections for core-valence correlation and relativistic effects. For the latter, we have developed and coded a variational treatment of nuclear motion that is based on the Hougen-Bunker-Johns approach with an Eckart-frame kinetic energy operator and thus also handles large amplitude motion. This has led to a general and robust variational code (TROVE) that was published in 2007 and has since been refined in several stages.

Over the past three years, the focus has been on the computation of comprehensive line lists for molecules of astrophysical interest, for example with regard to studies of the atmosphere of exoplanets (in collaboration with the Tennyson group at UCL). In this context, highly accurate ab initio potential energy surfaces were computed for methane [79], chloromethane [43], and silane [46], and ab initio dipole moment surfaces were generated for the latter two molecules [46, 78]. This enabled the simulation of accurate rovibrational spectra and the computation of extensive line lists. In the case of methane, sub-wavenumber accuracy was achieved for the majority of experimentally known vibrational energy levels, and the four fundamentals of $^{12}CH_4$ were reproduced with a root-mean-square error of 0.70 cm^{-1} [79]. In the case of chloromethane, the computed line lists for $CH_3{}^{35}Cl$ and $CH_3{}^{37}Cl$ cover vibrational band origins up to 4400 cm^{-1} and states up to J=85 [78]. As an illustrative example, Figure 1 documents the excellent agreement between the computed and observed spectrum for the ν_5 band of chloromethane. The line positions are again predicted with sub-wavenumber accuracy, and the computed absolute line intensities are accurate to a few percent [78].

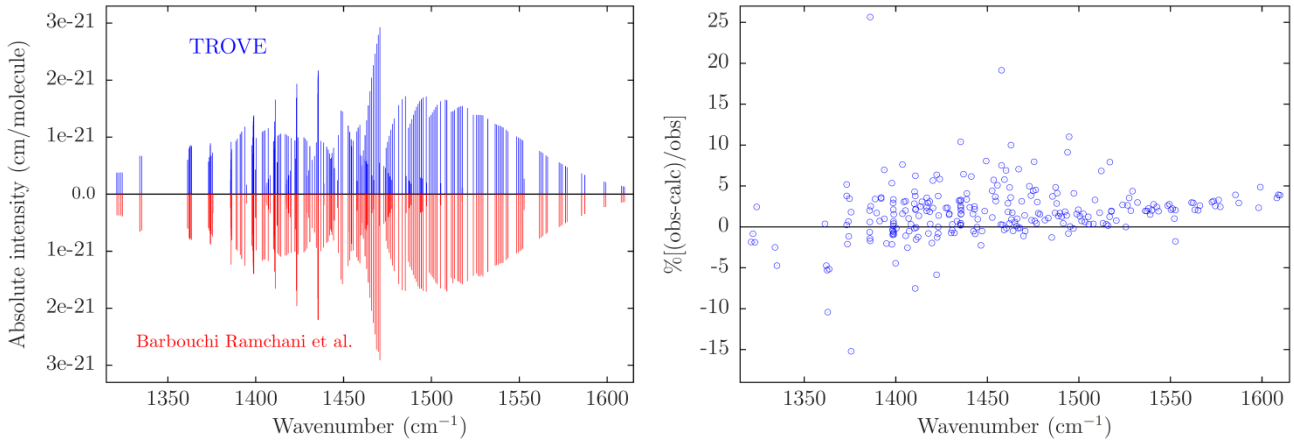

Fig. 1. Absolute line intensities of the ν_5 band of chloromethane for transitions up to J = 15 (left) and the corresponding residuals (right) when compared with measurements from Ramchani et al. Transitions for both $CH_3{}^{35}Cl$ and $CH_3{}^{37}Cl$ are shown and the intensities have not been scaled to natural abundance. For illustrative purposes TROVE line positions have been shifted by −0.40 cm^{-1} (from Ref. 78).

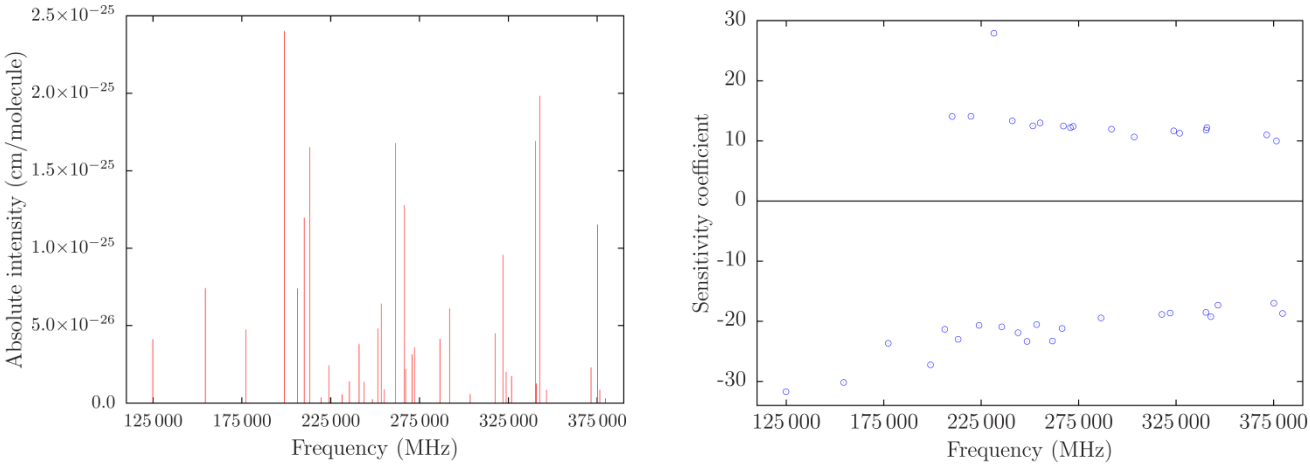

Fig. 2. Observed frequencies and simulated intensities at temperature T = 296 K (left panel) with the corresponding sensitivity coefficients (right panel) for transitions involving the $2\nu_2$ and ν_4 vibrational states of ammonia (from Ref. 77).

Experimentally, high-resolution rovibrational spectroscopy is accurate enough to allow for tests on fundamental theories of physics. In the search for a theoretical framework beyond the established Standard Model of Physics, there has been speculation that the natural constants may indeed not have remained constant over the entire age of the universe and that there may have been changes, for example, in the proton-to-electron mass ratio μ. This would lead to temporal shifts in rovibrational transition energies, which could be detected by high-precision laboratory experiments over a short time scale (say one year) or by astronomical observation of spectral lines at high red-shifts. Such measurements have already put rather tight constraints on the size of possible changes in μ. Theoretically, the effect of changes in μ can be determined through

TROVE calculations that employ suitably scaled mass values. Hence, it is possible to identify transitions that are particularly sensitive to changes in μ and thus especially promising for experimental study. We have performed such calculations for NH_3, H_3O^+, and D_3O^+ to determine the relevant sensitivity coefficients [44, 45, 77], and have indeed found a number of transitions with sensitivity coefficients that are significantly higher than those in the currently available best measurements on methanol. Our calculations indicate that the constraints on possible changes in μ may be tightened by about an order of magnitude by measuring these transitions in ammonia [77]. Figure 2 shows the frequencies and predicted selectivity coefficients of some of the most promising transitions in ammonia [77].

Further ab initio activities included a joint experimental and theoretical study on the high-resolution rovibrational spectrum of PF_3 [27] and a continuation of our ab initio benchmarks on electronically excited states using the SOPPA approach [47]. In comparative evaluations of the performance of computational methods, high-level ab initio calculations were carried out to generate reference data, for instance in studies of conical intersections [15] and of the reaction between FeO^+ and H_2, the prototypical example of two-state reactivity [1]. Finally, in our investigations of electronically excited states and electronic spectroscopy, correlated ab initio calculations (e.g. at the MS-CASPT2 level) were performed for comparison or validation on a regular basis in projects that mainly utilize lower-level methods (see the next chapters).

Publications resulting from this research area: 1, 4, 15, 27, 30, 43, 44, 45, 46, 47, 77, 78, 79

External funding: None

Cooperations: W.-H. Fang (Beijing, CN); F. Neese (Mülheim/Ruhr, DE); S. P. A. Sauer (Copenhagen, DK); V. Spirko (Prague, CZ); J. Tennyson (London, UK); S. N. Yurchenko (London, UK)

2.5.2 Research Area "Density Functional Methods" (W. Thiel)

Involved: G.-J. Cheng, D. Escudero, D. Fazzi, G. Gopakumar, P. Gupta, J. P. Götze, B. Heggen, B. Karasulu, C. Loerbroks, M. Patil, K. Sen, L. M. Wolf, Y. Zheng

Objective: Density functional methods are applied in studies of transition metal and other compounds in order to understand and predict their properties. Much of the work on homogeneous transition metal catalysis and organocatalysis involves a close collaboration with experimental groups at our Institute and aims at a detailed mechanistic understanding of the reactions studied experimentally. Time-dependent density functional theory is used in combination with other computational methods to interpret electronic spectra and to understand excited-state properties and processes.

Results: In many of our applications in this area, we employ state-of-the-art density functional theory (DFT) to explore the ground-state potential energy surface and to characterize all relevant intermediates, transition states, and reaction pathways. Geometry optimizations are normally done using standard functionals (RI-BP86, B3LYP) with dispersion corrections (D2, D3) and medium-size basis sets, followed by higher-level single-point energy evaluations that utilize either correlated ab initio methods (e.g., local CCSD(T) treatments with large basis sets) or modern density functionals (e.g., from the M06 series) with large basis sets and dispersion corrections (if appropriate). Effective core potentials are normally used to represent the core electrons of heavy elements. Thermal and entropic corrections are computed at the level applied for geometry optimization.

Joint projects with the Fürstner group: In continuation of a long-standing cooperation, we performed DFT calculations on the mechanism of catalytic reactions investigated experimentally in the Fürstner group [17, 34, 37, 52, 66]. An illustrative example is the Ru-catalyzed hydrogenation of internal alkynes that leads to the formation of ruthenium carbenes and of trans-alkenes, with minor amounts of side products (isomerized alkenes and alkanes) [37]. The DFT-based modeling of this reaction (precatalyst Cp*Rh(cod)Cl, substrate 2-butyne) provides a mechanistic scenario (Figures 3-5) that is consistent with all the experimental evidence (NMR, X-ray, product analysis) [37]. Oxidative addition of H_2 to the catalyst-substrate complex (**A1**) yields a dihydride (**A2**) that rearranges in a rate-limiting step to a η^1-vinyl complex (**A3**). Ring closure of **A3** involves twisting of the vinylic C=C double bond, which can occur in opposite directions and thus lead to two different ruthenacyclopropenes (**E1**, **Z1**) that are precursors to the trans-butene (**E2**)

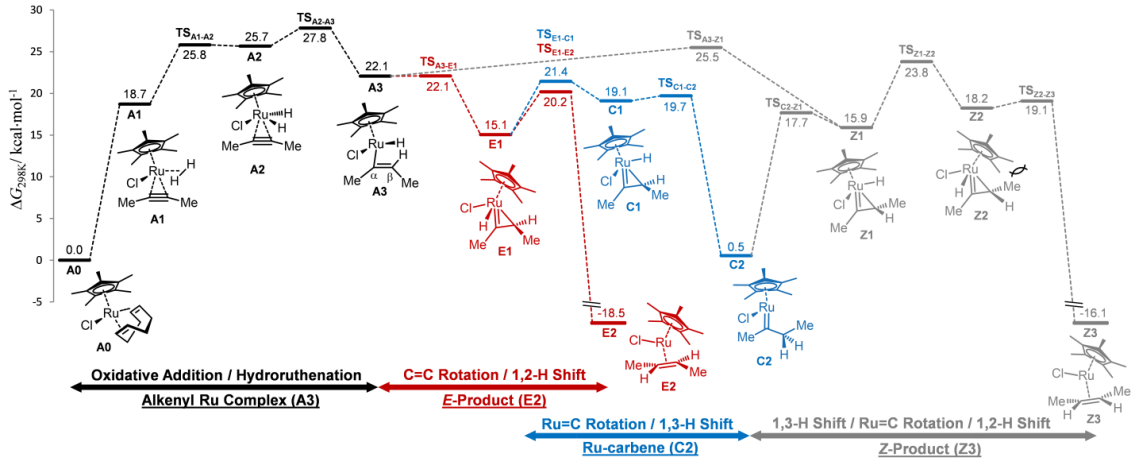

Fig. 3. Free energy profile for the hydrogenation of 2-butyne with complex **A0** at 298 K; computed structures of pertinent intermediates (from Ref. 37).

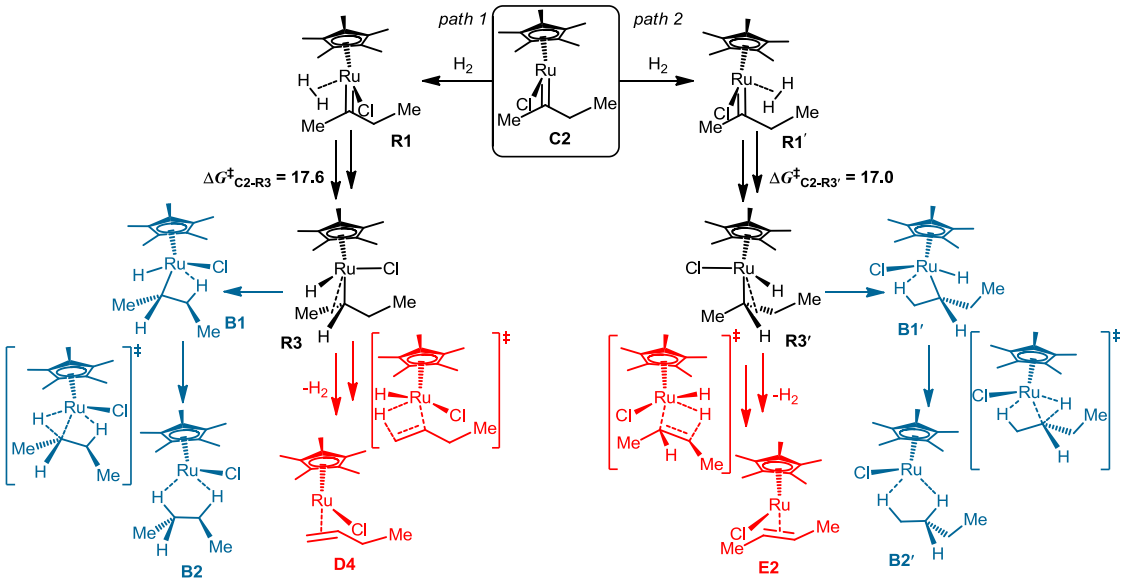

Fig. 4. Computed fate of the carbene formed by *geminal* hydrogenation upon addition of a second H_2 molecule (from Ref. 37).

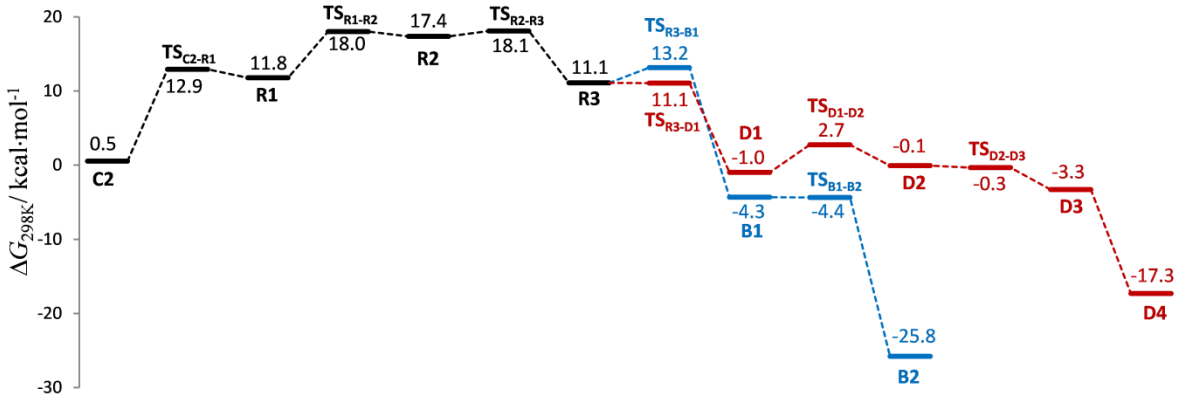

Fig. 5. Free energy profile for path 1 from the left side of Figure 4 at 298 K (from Ref. 37).

and cis-butene (**Z2**) product complexes. According to the computed free energy profile (Figure 3) the *trans/cis*-selectivity is determined by the relative ease of ring closure: $\mathbf{TS_{A3\text{-}E1}}$ is favored over $\mathbf{TS_{A3\text{-}Z1}}$ by more than 3 kcal/mol, consistent with the observed *trans*-hydrogenation. The ruthenium carbene (**C2**) is accessible from **E1** through an alternative rearrangement (involving Ru-C rotation) that requires only slightly more activation (ca. 1 kcal/mol) than the pathway to **E2**, in agreement with the observed formation of such carbenes. Various intramolecular transformations of carbene **C2** can be conceived, but none of the computed barriers is lower than that for the back-reaction to **E1**. However, **C2** can react with another molecule of H_2 (Figure 4), which provides a rather facile route to the observed side products, butane **B2** and 1-butene **D4** (Figure 5). Single-point coupled cluster calculations at the DLPNO-CCSD(T)/TZVP level confirm the validity of the DFT energy profiles (M06/TZVP, Figures 3-5), with minor changes in the computed energies of up to 2 kcal/mol (unpublished results by L. M. Wolf). To summarize, our combined experimental and computational approach has succeeded in rationalizing the preference for *trans*-hydrogenation and the unprecedented formation of ruthenium carbenes in our target system [37].

Having discussed the preceding DFT reactivity study at some length to convey a feeling of this type of collaborative work, we will be brief in the remainder of this section. A second major joint project concerned enantioinversion in gold catalysis [34]. In the cyclization of a hydroxy-allene to the corresponding tetrahydrofuran catalyzed by a TADDOL-related gold-phosphoramidite complex, it was found experimentally that the sense of induction can be switched from (*S*) to (*R*) solely by changing either the solvent or the temperature or the nature of the counterion; our DFT calculations provide a mechanistic scenario that allows us to rationalize these observations: key is the bias of the organogold intermediates to undergo assisted proto-deauration – a process strongly influenced by entropic effects that can ultimately dictate the stereochemical outcome [34]. Further computational DFT work on topics studied in the Fürstner group addressed the electronic structure and chemical bonding in hetero-bimetallic complexes obtained in attempts to prepare germane gold carbenoids devoid of stabilizing substituents via transmetalation [17], the NMR spectra and conformational preferences of mandelalide A and related compounds [52], and the mechanism of iron-catalyzed cross coupling reactions via ferrate intermediates [66]. Completed but still unpublished are mechanistic DFT studies on *trans*-hydrostannation (by L. M. Wolf) and on regio- and stereoselective Ru-catalyzed alkyne-alkene coupling (by G.-J. Cheng).

Joint projects with the Alcarazo group: The research in the Alcarazo group is directed towards the design and synthesis of unusual ligands and coordination compounds and their application in novel catalytic transformations. In our collaborative work, we perform DFT calculations to characterize the electronic structure of key species and to unravel the detailed mechanism of the catalytic reactions. In the reporting period, we addressed bis- and tris(pyrazolyl)borate/methane-stabilized P(III)-centered cations [9], the reactivity of tetrakis(trifluoromethyl)cyclopentadienone towards carbon-based Lewis acids [33], and the electronic properties of α-cationic arsines [60]. In the latter case, the DFT calculations also helped elucidate the mechanism of cycloisomerization of enynes to cyclopropanes, catalyzed by novel Pt(II) complexes containing α-cationic arsines as ligands [60]. Furthermore, DFT results are available from another joint project that addresses α-dicationic phosphines and their role as ligands in the Rh-catalyzed hydroarylation of dienes with electron-rich aromatic molecules (work by L. M. Wolf, manuscript submitted).

Joint projects with the List group: The collaboration with the List group in the field of organocatalysis has intensified during the reporting period, as shown by a growing number of publications [38, 57, 65, 72, 75, 90]. Following the development of a highly enantioselective carbonyl-ene cyclization using a confined imidodiphosphate catalyst, ESI-MS, NMR, and DFT studies were combined to unravel the mechanism of this reaction, which proceeds stepwise and involves a novel covalent intermediate [38]. In a similar vein, DFT calculations provided insight into the mechanism of the asymmetric oxa-Pictet-Spengler reaction catalyzed by nitrated confined imidophosphates [57]. DFT modeling was also used to elucidate the origin of the unusually high *trans*-diastereoselectivity of the chiral imidodiphosphoric acid-catalyzed Prins cyclization reaction [90]. After establishing heterodimerizing self-assembly between a phosphoric acid catalyst and a carboxylic acid as a new activation mode in Brønsted acid catalysis, the underlying mechanism was investigated both experimentally and theoretically; the DFT calculations served to characterize the nature of the supramolecular heterodimer and to rationalize the observed catalyst structure-selectivity relationships [75]. Further DFT investigations addressed the nature of the transition state in the catalytic 6π electrocyclization of unsaturated hydrazones [65] and the CD spectra of enantiopure 2*H*- and 3*H*-pyrroles synthesized by a novel organocatalytic approach [72].

Joint project with the Maulide group: The collaboration with the Maulide group has been phased out in view of their move to the University of Vienna. Our final joint paper concerns the dynamic behavior of internally coordinated monohaptoallylpalladium

complexes [54]. DFT modeling was used to characterize the investigated cyclobut-2-enyl η^1-allyl palladium complexes and to elucidate the detailed mechanism of the metallotropic shift in these systems (stepwise π-σ-π interconversion) [54].

Joint project with the Klussmann group: Our first collaborative project with the Klussmann group addressed the question whether hydrogen atom transfer (HAT) or electron transfer (ET) is the key step in the activation of *N*-aryl tetrahydroisoquinolines in oxidative coupling reactions using CuBr as catalyst and *tert*-butyl hydroperoxide [55]. The combined experimental and computational evidence clearly favors the HAT mechanism. The DFT calculations contributed a computational Hammett plot analysis, predictions of kinetic isotope effects, and free energy profiles for competitive HAT reactions involving the *t*BuO· and *t*BuOO· radicals [55].

Joint projects with the Rinaldi and Schüth groups: These projects on biomass conversion had started in the previous reporting period and have meanwhile been finished. The focus was on the computational modeling of the depolymerization of cellulose to glucose. The initial DFT results for cellobiose (glucose dimer) had shown that cellulose is protected against hydrolysis not only by its supramolecular structure (as commonly accepted), but also by its electronic structure (especially the anomeric effect). Subsequent DFT/MM calculations on the depolymerization of larger cellulose models (up to 40 linked glucose units) in water confirmed the basic mechanistic features deduced from the initial DFT study, while providing detailed information on the influence of nearby solvent molecules [40]. Classical molecular dynamics and metadynamics simulations of these larger models in water and in a ionic liquid indicate that the latter eases hydrolysis through stronger solvent-cellulose interactions and that hydrolysis should start from the ends of cellulose chains [39]. In a related project, the isomerization of glucose to fructose in water was studied at the DFT level to clarify the detailed reaction mechanism and to rationalize the observed differences in the catalytic efficiency of different metal cations [12].

Other ground-state DFT projects: Some ground-state DFT studies have been carried out without involvement of experimental groups from the Institute [11, 24, 48, 67, 80]. These include detailed investigations on the origin of the stereochemical preferences (inversion versus retention) in the oxidative addition step of Pd-catalyzed allylic alkylation [24], on the influence of halogen bonding on the spin state of diphenylcarbene [67], and on the mechanism of ylide transfer to carbonyl compounds using two different sulfur reagents [80].

Electronically excited states: Our research on electronically excited states makes use of the full arsenal of quantum-chemical methods. In the realm of DFT, we mostly rely on time-dependent density functional theory (TD-DFT) and on DFT-based multireference configuration interaction (DFT/MRCI). In the following, we summarize studies on excited states that were mainly carried out at the DFT level (possibly in combination with some ab initio calculations), while we do not cover DFT-based calculations that were done for comparison or validation purposes in our semiempirical excited-state dynamics work (see the next chapter).

Excited-state DFT projects: The performance of DFT/MRCI and several TD-DFT schemes (pure, hybrid, and long-range corrected functionals) was assessed for a set of 3*d* and 4*d* transition metal complexes, by comparing against high-level ab initio reference data for transition energies and oscillator strengths; DFT/MRCI performed best [5]. DFT/MRCI also gave satisfactory results for the spectroscopic and second-order nonlinear optical properties of selected Ru(II) complexes [30]. Different Franck-Condon methods for computing vibrationally broadened UV-Vis absorption spectra were implemented and assessed for flavin derivatives in order to set up a protocol with recommended options [10]. The photoinduced intramolecular charge transfer (ICT) was investigated at the TD-DFT (CAM-B3LYP) and DFT/MRCI levels for roseoflavin, a push-pull flavin derivative, in different environments; the perpendicular-twisted ICT mechanism was found to be favored [35]. A DFT-based computational screening of flavin derivatives absorbing in the blue-green region revealed that certain thioflavins are potentially suitable candidates as cofactors in biomimetic photoswitches [14]. An analysis of the excited-state energy levels of two carotenoids (violaxanthine, zeaxanthine) from TD-DFT (CAM-B3LYP) and DFT/MRCI suggested that carotenoids may act as a shortcut for chlorophyll Soret-to-Q band energy flow in the light-harvesting complex LHCII [8]. The exploration of the relevant triplet excited-state potential energy surfaces of a cyclometalated Pt(II) complex at the TD-DFT level (with inclusion of spin-orbit coupling) indicated non-Kasha behaviour (Figure 6), i.e. emission from a higher-lying triplet state [6]. The mechanism for catalytic photooxidation of benzene to phenol with 2,3-dichloro.5,6-dicyano-*p*-benzoquinone (DDQ) was found to involve nonadiabatic orientation-dependent proton-coupled electron transfer processes [28]. Finally, the mechanism of the [2+2] photocyclization of atropisomeric maleimides was elucidated in detail through DFT calculations, which rationalize the observed regioselectivity as well as the substituent effects on enantioselectivity and diastereoselectivity [56].

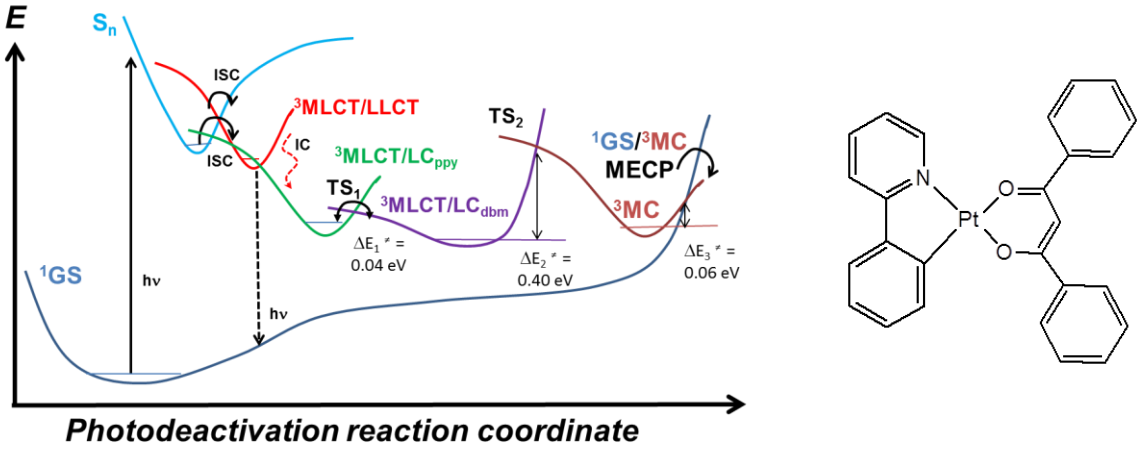

Fig. 6. Schematic Jablonski diagram for the Pt complex shown on the right, including the lowest-energy states involved in the proposed radiative and non-radiative deactivation pathways (from Ref. 6).

Photovoltaics: Our recent DFT-based research on photovoltaics (in collaboration with M. Barbatti) has led to three computational papers [19, 31, 62] and four collaborative publications with external experimental partners [13, 69, 74, 86]. The first study addressed the electronic structure and electronic spectra of three squaraine dyes and their donor-acceptor complexes with fullerene C_{60}. For these complexes, the measured open-circuit voltage is correlated to the charge-transfer energy, and anticorrelated to the energy of the first excited state, which can be rationalized by a simple non-Marcus model [19]. The other two computational studies involved excited-state dynamics simulations of oligothiophenes (300 fs) using trajectory surface hopping (TSH) at the TD-DFT level. The intramolecular dynamics in a tetrathiophene chain leads to exciton localization over three repeat units after ca. 140 fs, consistent with experimental observations in polymers [31]. Photoexcitation into the high-energy (HE) band of a dithiophene dimer generates hot charge transfer states within ca. 50 fs, but the subsequent ultrafast decay to the low-energy (LE) states causes localization of the excitation at one monomer followed by internal conversion to the ground state with C-S bond cleavage [62]. This suggests that the lifetime of the hot excitons (favoring charge transfer and ultimately charge separation) might be increased by designing functionalized aggregates with a higher HE-LE energy gap (disfavoring exciton transfer to the LE regime) [62]. In the collaborative projects with experimentalists, the DFT calculations provided insight into the structure-function relationships of high-electron mobility naphthalene diimide copolymers [13], into the polaronic properties of narrow band gap polymers [69] and n-doped ladder-type conducting polymers [86], and into the electronic structure of carbazole-containing copolymers used in solar cells [74].

Reviews: Surveys of DFT studies are given in reviews on computational catalysis [23] and on excited-state methods [68].

Publications resulting from this research area: 5, 6, 8-15, 17, 19, 23, 24, 28, 30, 31, 33, 34, 35, 37, 38, 48, 52, 54-57, 60, 62, 65-69, 72, 74, 75, 80, 86, 90

External funding: Cluster of Excellence RESOLV (DFG), SusChemSys (NRW)

Cooperations: M. Alcarazo (Mülheim/Ruhr, DE); M. Barbatti (Mülheim/Ruhr, DE); A. G. M. Barrett (London, UK); C. J. Brabec (Erlangen, DE); B. Champagne (Namur, BE); S. Fabiano (Linköping, SE); W.-H. Fang (Beijing, CN); A. Fürstner (Mülheim/Ruhr, DE), M. Klussmann (Mülheim/Ruhr, DE); M. A. Loi (Groningen, NL); B. List (Mülheim/Ruhr, DE); C. M. Marian (Düsseldorf, DE); N. Maulide (Mülheim/Ruhr, DE); T. C. Ramalho (Lavras, BR); E. Sánchez-García (Mülheim/Ruhr, DE); W. Sander (Bochum, DE); F. Schüth (Mülheim/Ruhr, DE); M. Sommer (Freiburg, DE)

2.5.3 Research Area "Semiempirical Methods" (W. Thiel)

Involved: G. Cui, P. Dral, J. A. Gámez, B. Heggen, A. Koslowski, Z. Lan, J. Liu, Y. Lu, A. Nikiforov, A. Rodriguez, N. Sahu, L. Spörkel, D. Tuna, X. Wu

Objective: This long-term project aims at the development of improved semiempirical quantum-chemical methods that can be employed to study ever larger molecules with useful accuracy. This includes the development of more efficient algorithms and computer programs. Our current focus in this area is on the development of improved orthogonalization-corrected methods and on non-adiabatic dynamics simulations of electronically excited states.

Results: Over the past years, we have developed semiempirical methods that go beyond the standard MNDO model by including orthogonalization corrections at the NDDO level. This has led to three new approaches labelled OM1, OM2 and OM3 (orthogonalization models 1-3) that offer significant improvements over established MNDO-type methods in several areas, including conformational properties, hydrogen bonds, reaction barriers, and electronically excited states.

In the reporting period, the underlying theoretical formalism, the implementation, and the parametrization of the OMx methods were described in full detail [58]. This paper also addressed the efficiency of the OMx code on different hardware platforms and the use of *a posteriori* dispersion corrections for a much improved treatment of noncovalent interactions (OMx-Dn approach) [58]. In a companion publication, the performance of the OMx and OMx-Dn methods was evaluated for a variety of ground-state properties using a large and diverse collection of benchmark sets from the literature, with a total of 13035 reference data [59]. Extensive comparisons with established semiempirical methods show that the OMx and OMx-Dn methods outperform the other methods for most of the benchmark sets by a significant margin [59]. Similar comprehensive evaluations of the OMx/MRCI methods were carried out for electronically excited states, covering vertical and adiabatic excitation energies, excited-state equilibrium geometries, minimum-energy conical intersections, and excited-state zero-point vibrational energies, for a total of 520 molecular structures and 412 excited states [82]. Comparisons with high-level ab initio and TD-DFT reference data indicate that the OMx/MRCI methods perform reasonably well for many of the excited-state properties [82]. This paper also summarizes recent improvements of our semiempirical MRCI code, which include the implementation of a shape-driven version of the GUGA-CI

algorithm (GUGA, graphical unitary group approach) and of a direct variant of the code (with the CI coupling coefficients being recomputed as needed) [82].

Ongoing work addresses the further development and refinement of the OMx methods. This includes the theoretical analysis of the existing formalism, the design and test of new integral approximations, the improvement of parametrization techniques, the assembly of suitable reference data, and the actual parameterization of the refined OMx methods for as many elements as possible. Progress has been made on all these fronts. It is clear that the next generation of OMx methods will have fully integrated dispersion corrections (rather than an *a posteriori* treatment). New integrals approximations are being developed, e.g., for the resonance integrals. Our arsenal of parametrization methods has been supplemented with machine learning techniques [29]. Extensive high-level reference data for ground-state and excited-state properties are available from our recent benchmark studies [58, 59, 82]. In view of the excellent performance of the OMx methods for first-row elements, their parametrization is being extended to second-row elements (even though the use of an *sp* basis will not allow meaningful calculations for hypervalent compounds); the OM2 parametrization for sulfur is finished and yields superior results for normalvalent compounds (manuscript in preparation). Furthermore, parametrizations of next-generation OMx methods with fully integrated dispersion corrections have been performed for first-row elements, and the currently available results already present significant improvements in overall accuracy. Finally, a large number of test parametrizations are being run to assess the merits and shortcomings of new integral approximations. Much of this is rather tedious work, which is however necessary to develop general-purpose next-generation semiempirical methods with improved overall performance.

Over the past three years, our semiempirical applications have focused on excited-state dynamics. We had previously implemented the trajectory surface hopping (TSH) method with the fewest switches algorithm (Tully) in our software, making use of our semiempirical in-core version of the GUGACI method that handles general CI expansions (up to full CI) efficiently for small active spaces and provides an analytic GUGACI gradient as well as analytic nonadiabatic coupling matrix elements. Technical problems may arise in such TSH simulations with a predefined active space whenever active and inactive orbitals strongly mix and switch in some particular regions. We have largely overcome these problems by employing adaptive time steps when such regions are encountered in TSH simulations [81]. The corresponding computational protocol is easy to implement and increases the computational effort only in the critical regions;

tests on a GFP chromophore model and a light-driven rotary molecular motor show that the number of successful trajectories without technical failures rises significantly by the use of adaptive time steps, from 53 % to 95 % and from 25 % to 96 %, respectively [81]; this is now the default option in TSH simulations. Another methodological advance is a generalization of the TSH method by including spin-orbit coupling, thus allowing the simulation of both internal conversion and intersystem crossing on an equal footing; our implementation considers hops between adiabatic eigenstates of the non-relativistic electronic Hamiltonian (pure spin states), which is appropriate for sufficiently small spin-orbit coupling [4].

Most of our excited-state dynamics studies were carried out at the OM2/MRCI level for medium-size organic molecules in the gas phase. These TSH simulations provided insight into the origin of the enhanced $E \rightarrow Z$ photoisomerization in 2-aminoazobenzene [7], the nonequilibrium H/D isotope effects in excited-state intramolecular proton transfer (ESIPT) processes [21], the photochromism and photoswitching potential of a prototypical Schiff base, salicylidene methylamine [50], the dynamics of an unusual excited-state proton transfer to a carbon atom [53], the enhancement of the fluorescence emission of a locked GFP chromophore by ESIPT-induced trapping of a keto tautomer [73], the computational design of a family of light-driven rotary molecular motors with improved quantum efficiency [76], and the stereospecific unidirectional excited-state relaxation during the photoisomerization of arylazopyrazole photoswitches [87]. The results of these OM2/MRCI studies are generally consistent with the available experimental data and high-level static calculations, but the dynamics simulations often detect pathways and preferences between pathways that are not obvious from the static calculations. These successful applications corroborate the previously available evidence that the OM2/MRCI approach is a suitable tool for investigating the excited states and the photochemistry of large molecules.

For the sake of brevity, it is not possible to discuss all these dynamics studies in detail. Instead we comment on one illustrative example, the photodynamics of GFP model chromophores (Figures 7-8), in order to convey a feeling of the types of results that can be obtained. The native GFP chromophore (p-HBDI in Figure 8) has a *para*-hydroxyl group at the phenyl ring. The *ortho*-isomer (o-HBDI in Figure 8) and the locked *ortho*-isomer (o-LHBDI in Figure 8) have been synthesized and characterized experimentally. Photoexcitation of p-HBDI triggers photoisomerization around the central C=C bond with fast deactivation to the ground state. Excited-state dynamics simulations show that this photoisomerization cannot compete with the ultrafast ESIPT process in o-HDBI and

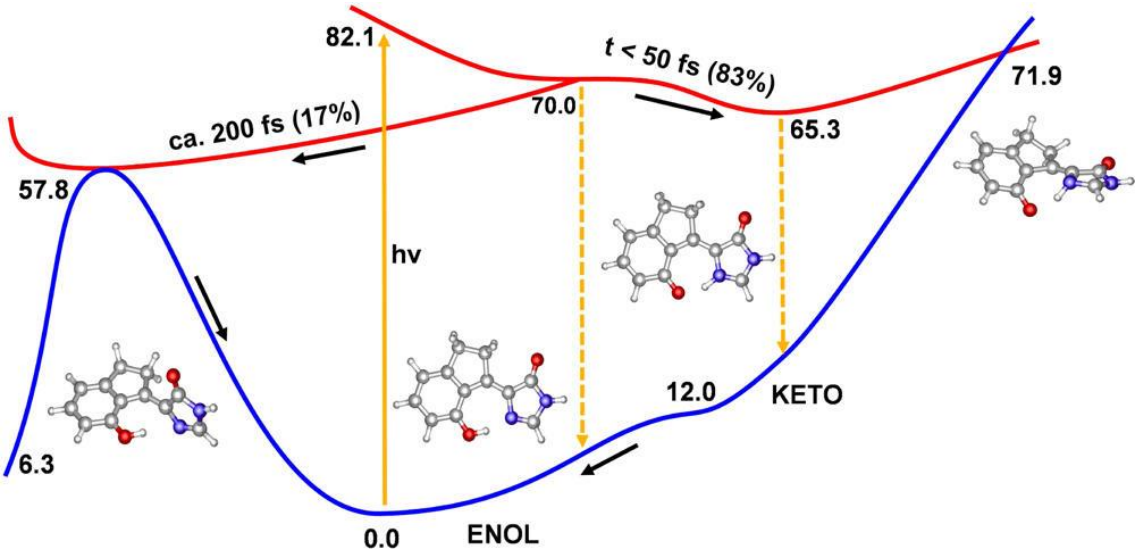

Fig. 7. Photochemical mechanism derived from static electronic structure calculations and nonadiabatic dynamics simulations of o-LHDBI (from Ref. 73).

Note: According to the TSH simulations, photoexcitation of the stable ground-state enol tautomer of o-LHDBI to the S_1 state triggers an ultrafast ESIPT process that populates the keto tautomer within 50 fs (83 %), with a minor fraction of the trajectories (17 %) reaching the enol-type conical intersection with the ground state within ca. 200 fs. The route from the S_1 keto form to the keto-type conical intersection with the ground state is uphill, and hence the S_1 keto form is trapped long enough to fluoresce.

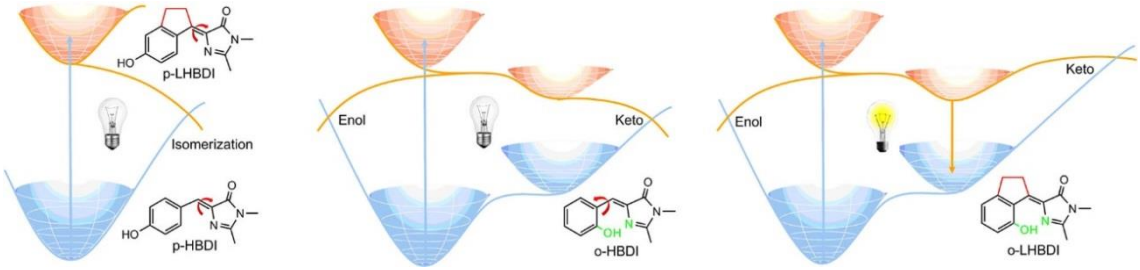

Fig. 8. Comparison of photophysical and photochemical mechanisms of three types of GFP core chromophores. p-HBDI and p-LHBDI are non-emissive in vacuo and solution due to excited-state deactivation induced by cis-trans isomerization. o-HBDI is non-emissive because of ESIPT-induced excited-state deactivation. In o-LHBDI, ESIPT leads to an excited-state trapping that enhances the ability of the S_1 keto species to fluoresce (from Ref. 73).

o-LHDBI, which yields the excited-state keto tautomer (enol/keto tautomerization). They also indicate that the conical intersection with the ground state can thereafter be reached easily in o-HDBI, but not in o-LHDBI because of the chemical locking by the extra five-membered ring, which impedes the required out-pf-plane distortions. The TSH simulations thus rationalize the different photophysical behavior of the three GFP model chromophores considered [73].

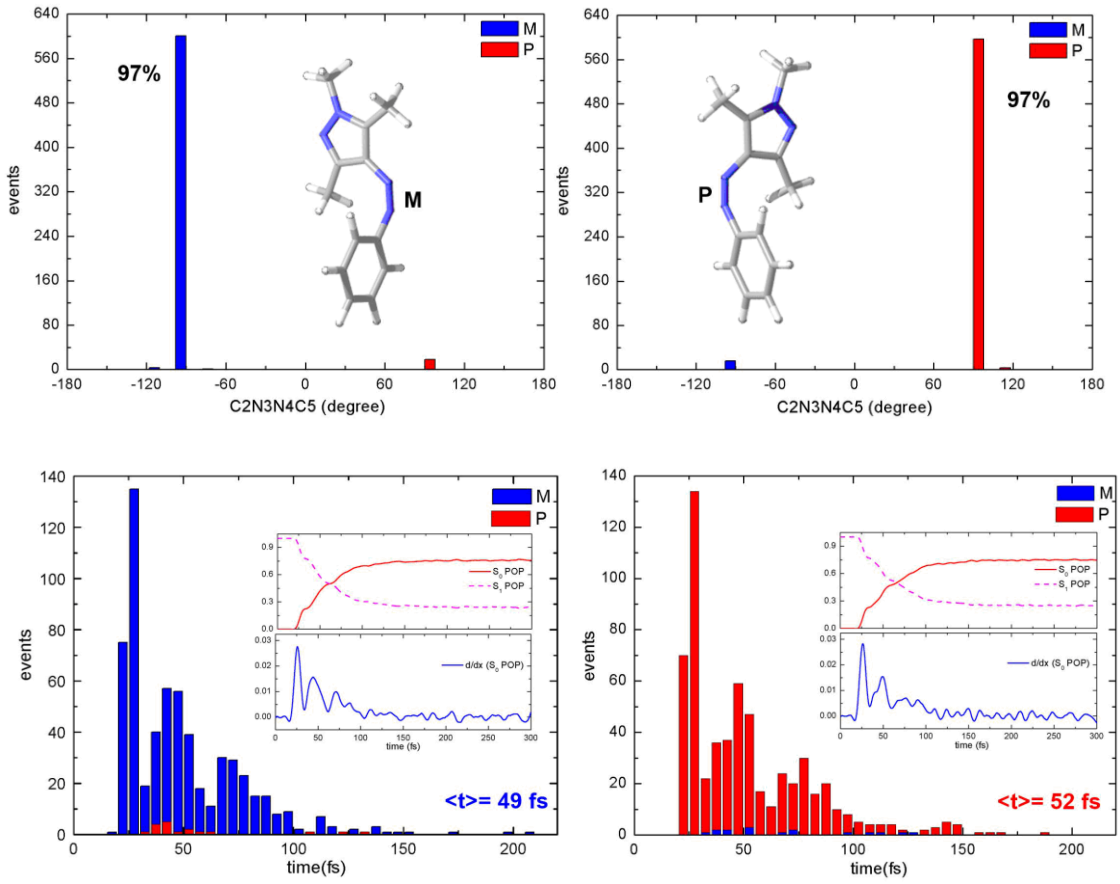

Fig. 9. Distribution of (top) the C2N3N4C5 dihedral angles and (bottom) the hopping times at all $S_1 \rightarrow S_0$ hopping points, with time-dependent state populations and their time derivatives (insets). Left panels, trajectories starting from the M enantiomer (S_0); right panels, trajectories starting from the P enantiomer (S_0). Hops through the M conical intersection (S_1S_0) in blue, hops through the M conical intersection (S_1S_0) in red (from Ref. 87).

A second illustrative example is provided an azo compound (denoted as Z11), in which the central N=N double has one phenyl and one trimethylpyrazolyl substituent (see Figure 9). Like azobenzene itself, the *cis*-isomer of arylazopyrazole Z11 exists in two helical forms (M and P). The *cis/trans*-photoisomerization of Z11 can in principle occur in two different ways, with opposite sense of rotation. The TSH simulations show unidirectional dynamical behavior, with an overwhelming majority of the trajectories retaining the helicity in the preferred mode of rotation (97 %). To our knowledge, this is the first case of an essentially stereospecific excited-state relaxation [87].

Reviews and benchmarks: Recently we published reviews on semiempirical methods in general [22], on the computational modeling of photoexcitation in DNA single and double strands [41], and on the use of graphical processing units for fast semiempirical calculations [88]. A benchmark study confirmed the satisfactory performance of the OM2/MRCI method for conical intersections in organic molecules, through comparisons with ab initio MRCI and DFT-based methods [15].

Future directions: Research in the framework of the ERC Advanced Grant will focus on the further development and application of OMx methods. This includes the reparameterization of the existing OMx methods with inclusion of dispersion corrections aiming at a balanced treatment of ground-state and excited-state properties, the reformulation of the OMx methods with the use of different types of integral approximations to facilitate the extension to heavier main-group elements and transition metals with an *spd* basis, and generic as well as specific parameterizations for transition metals. Semiempirical applications will concentrate on excited states of large complex systems (spectroscopy, photochemistry, solar cells) using both static calculations and dynamics simulations.

Publications resulting from this research area: 4, 7, 15, 21, 22, 26, 29, 41, 50, 53, 58, 59, 64, 73, 76, 81, 82, 87, 88

External funding: ERC Advanced Grant (European Research Council)

Cooperations: M. Elstner (Karlsruhe, DE); W.-H. Fang (Beijing, CN); M. Filatov (Bonn, DE); A. Lübcke (Berlin, DE); O. A. von Lilienfeld (Basel, CH)

2.5.4 Research area "Combined Quantum Mechanical / Molecular Mechanical Methods and Classical Dynamics" (W. Thiel)

Involved: E. Boulanger, G. Cui, A. Escorcia Cabrera, A. Ganguly, J. P. Götze, S. Hare, B. Heggen, B. Karasulu, G. König, C. Loerbroks, M. Patil, T. Saito, K. Sen, P. Sokkar, J. van Rijn, T. Vasilevskaya, Y. Zheng

Objective: This research focuses on hybrid approaches for large systems where the active center is treated by an appropriate quantum mechanical method and the environment by a classical force field. It involves considerable method and code development. This approach allows a specific modeling of complex systems such that most of the computational effort is spent on the chemically important part. Current applications primarily target biocatalysis and aim at a better understanding of enzymatic reactions including the role of the protein environment, but also address solvation and excited-state processes.

Results: Combined quantum mechanical/molecular mechanical (QM/MM) methods are a popular tool for studying reactions in complex systems such as enzymes. In the preceding reporting periods, we had implemented polarizable force fields in this framework (QM/MMpol) and extended the two-layer QM/MM approach to a three-layer model by introducing boundary potentials that represent the outer part of the MM region and the bulk solvent. We have further refined the QM/MMpol scheme (by improving the treatment of the Drude oscillators and of the QM/MMpol boundary) and assessed its performance for small model systems and for the enzymatic reactions in chorismate mutase (CM) and p-hydroxybenzoate hydroxylase (PHBH), where inclusion of MM polarization affects the computed barriers by about 10 % [2]. As an alternative three-layer scheme, we have developed (in collaboration with E. Sánchez-García) a triple-resolution QM/MM/CG approach for biomolecular systems, in which the outermost layer is represented by the coarse-grained (CG) Martini force field [49]. Tests on the enzymatic reactions in CM and PHBH show that it is important to use an atomistic representation of the water molecules inside the enzyme and in the surface layer (up to at least 5 Å). Hence, the CG force field should only be applied for the bulk solvent, which limits the gains in computational efficiency [49]. The merits of various two-layer and three-layer approaches have been assessed more recently in systematic free energy calculations on CM and PHBH (unpublished work by A. Ganguly).

Most of the published QM/MM work on enzymes makes use of a finite droplet model, with the enzyme being embedded in a sufficiently large water sphere. An alternative is the QM/MM-Ewald approach with periodic boundary conditions (PBC) that evaluates

long-range electrostatic interactions properly by Ewald summation techniques. We have implemented the original semiempirical QM/MM-Ewald scheme proposed by Nam, York, and Gao (*J. Chem. Theory Comput.* 2005, *1*, 2). In addition, we introduced a generalized method (Gen-Ew) for periodic QM/MM calculations that can be used with any QM method in a QM/MM framework [85]. The Gen-Ew approach approximates the QM/MM-Ewald method by representing the PBC potential by virtual charges on a sphere and the QM density by electrostatic potential charges. The deviations between Gen-Ew and QM/MM-Ewald results are generally small enough to justify Gen-Ew applications. The results from periodic QM/MM energy and free energy calculations (QM/MM-Ewald, Gen-Ew) were compared to their nonperiodic counterparts (droplet model) for five test reactions in water and for the Claisen rearrangement in CM; excellent agreement was found in all cases, indicating that long-range electrostatic interactions are well captured by nonperiodic QM/MM calculations in a water droplet of reasonable size (radius of 15-20 Å) [85].

We now turn to recent QM/MM applications. In QM/MM studies on enzymatic reaction mechanisms, we normally use geometry optimization techniques to follow conceivable pathways on DFT/CHARMM potential energy surfaces in order to determine the most favorable one. Optimizations are normally done with efficient DFT approaches (e.g., RI-BP86 with moderate basis sets), while relative energies are determined using more refined functionals (e.g., B3LYP-D3 or M06 with larger basis sets) or even correlated ab initio methods (CCSD(T) or multi-reference treatments). If necessary, QM/MM free energy calculations are performed to include entropic contributions. In the following, we first describe one such mechanistic QM/MM study in some detail and then briefly summarize several others.

As illustrative example, we address amine oxidation mediated by *N*-methyltryptophan oxidase (MTOX) [36]. Amine oxidation is the rate-determining step in the three-step demethylation of *N*-methyltryptophan (NMT) catalyzed by MTOX, which employs a covalently bound flavin adenine dinucleotide (FAD) as cofactor. For the required transfer of a hydride ion equivalent, three pathways (direct/concerted, radical, and adduct-forming/polar nucleophilic) have been proposed (Figure 10), without a consensus on which one is commonly used by amine oxidases. We have combined theoretical pK_a analysis, classical MD simulations, pure QM calculations on active-site models, and QM/MM calculations on the full solvated enzyme (Figure 11) to provide molecular-level insights into the catalytic mechanism of NMT oxidation and to analyze the role of MTOX active-site residues and covalent FAD incorporation for NMT binding and oxidation. The QM(B3LYP-D2/6-31G(d))/CHARMM results clearly favor a direct concerted hydride transfer mechanism involving anionic NMT as the reactive

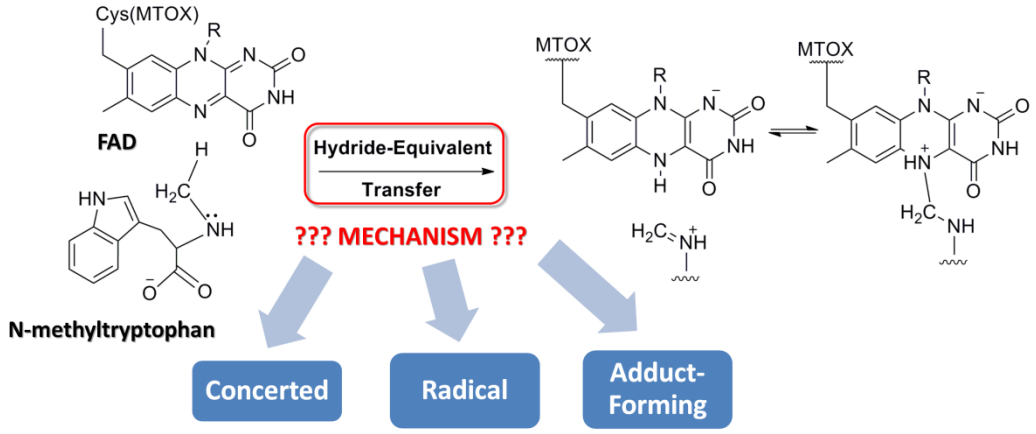

Fig. 10. Mechanistic alternatives for amine oxidation in MTOX (from Ref. 36).

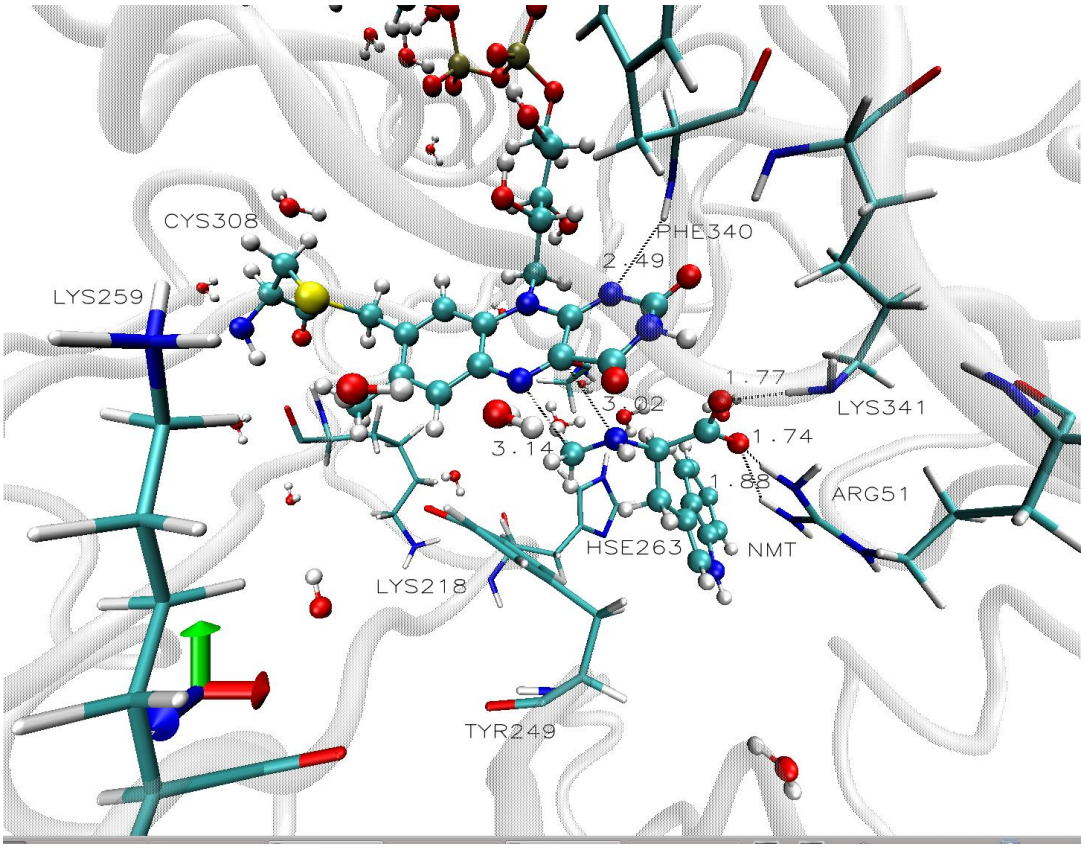

Fig. 11. Typical starting structure for QM/MM modeling of amine oxidation in MTOX, taken from an MD snapshot of the NVT ensemble for anionic *N*-methyltryptophan (K259: protonated, K341: deprotonated). Depicted are FAD and NMT (ball-and-stick), important MTOX residues (stick), and the MTOX structure (cartoon) (from Ref. 36).

species. On the basis of classical canonical MD simulations and QM/MM calculations of wild-type MTOX and two mutants (K341Q and H263N), we propose that the K341

residue acts as an active-site base and electrostatically, whereas H263 and Tyr249 only support substrate alignment. Covalent FAD binding leads to a more bent isoalloxazine moiety, which facilitates the binding of anionic NMT but increases the catalytic activity of FAD only slightly. Our computational results thus provide a detailed and consistent mechanistic scenario for amine oxidation in MTOX [36].

In the following, we briefly summarize the results from several other QM/MM studies on ground-state enzymatic reactions that were carried out during the reporting period.

The reversible oxygen binding in *hemocyanin*, a copper-containing enzyme, was studied at the QM/MM level using a broken-symmetry DFT treatment with spin projection corrections for the QM region [16]. The X-ray structures of the deoxygenated and oxygenated hemocyanin are well reproduced by QM/MM geometry optimizations. The oxygen binding proceeds stepwise with two sequential electron transfer (ET) processes in the triplet state followed by an intersystem crossing to the singlet product. The first ET step leads to a nonbridged superoxo $Cu_B^{II}–O_2•^-$ intermediate via a low-barrier transition state. The second ET step is even more facile and yields a side-on complex with the characteristic Cu_2O_2 butterfly core, accompanied by triplet-singlet intersystem crossing. The computed barriers are very small so that the two ET processes are expected to very rapid and nearly simultaneous [16].

For the *cytochrome P450EryF* enzyme, we investigated the role of two alternate water networks in the formation of the reactive Compound I (Cpd I) species [18]. MD simulations suggest the existence of two water networks around the active site, the one found in the crystal structure involving E360 and another one involving E244. According to the QM/MM calculations, the first proton transfer that converts the peroxo to the hydroperoxo intermediate (Compound 0, Cpd 0) proceeds via the E244 water network with direct involvement of the 5-OH group of the substrate. For the second proton transfer from Cpd 0 to Cpd I, the computed barriers for the rate-limiting homolytic O−O cleavage are similar for the E360 and E244 pathways, and hence both glutamate residues may serve as proton source in this step [18].

For the zinc-containing *matrix metalloproteinase-2* (MMP-2) enzyme, we explored the mechanism of peptide hydrolysis using the oligopeptide Ace-Gln-Gly~Ile-Ala-Gly-NMe as substrate [51]. The four-step mechanism involves an initial nucleophilic attack followed by hydrogen bond arrangement, proton transfer, and C-N bond cleavage. The computed QM/MM barriers for these chemical steps are quite low, and it thus seems likely that product release is rate-limiting in MMP-2 catalysis; this notion is supported by QM/MM reaction path calculations and steered MD simulations for the release

process [51]. In follow-up studies, we addressed the dependence of the QM/MM results on the chosen computational protocol (keywords: initial sampling, thickness of the solvent shell, energy versus free energy calculations) and the origin of the lower catalytic activity of the Glu116Asp mutant [83, 84].

In the area of ground-state enzyme reactivity, we have also published reviews on QM/MM studies of cytochrome P450 enzymes [20] and on computational biocatalysis in general [23]. In ongoing mechanistic QM/MM work (with A. Escorcia Cabrera and J. van Rijn) we investigate the origin of the enantioselectivity of the *Candida antarctica* lipase B (CalB) catalyzed *O*-acetylation of (*R*,*S*)-propranolol [61] and the mechanism of carbocation rearrangements in terpene synthases (manuscripts in preparation).

Turning to QM/MM projects on electronically excited states, we have studied the electronic absorption spectra and the photoinduced processes and reactions in a number of biomolecular systems. In comprehensive QM/MM work on channelrhodopsin-2 wild-type (ChR-WT) and the C128T mutant, the OM2/MRCI method was used with success to simulate the absorption spectra of Chr-WT and C128T as well as several related systems (retinal isomers, bacteriorhodopsin) [64]. In a QM/MM study of the light-harvesting peridinin-chlorophyll a-protein, DFT-based methods were used to compute the relevant excited-state structures, energies, and transition dipole moments, which allowed us to propose an energy transfer model that invokes vibrational relaxation in the lowest two singlet excited states as driving force for wavelength conversion [32]. DFT/MM simulations of phenylbenzothiazole compounds bound to a tyrosine kinase show that excited-state proton transfer can tune the emission properties of these molecules through differences in hydrogen bonding, which suggests the possibility of creating two-color fluorescent markers for protein binding sites [42]. According to QM(CASPT2//CASSCF)/MM calculations on the S65T/H148D double mutant of wild-type green fluorescent protein, the Asp148 residue drives the ultrafast formation (< 175 fs, barrierless ESIPT process) of the anionic fluorescent state (S_1 keto tautomer) that is then quickly deactivated through a concerted asynchronous hula-twist photoisomerization; this explains the low fluorescence quantum yield observed experimentally [25]. Finally, classical MD as well as ab initio QM/MM nonadiabatic dynamics simulations were used to model the photoinduced folding and unfolding processes in the azobenzene cross-linked FK-11 peptide; the interactions between the peptide and the azobenzene cross-linker were found to be crucial for controlling the evolution of the secondary structure of the peptide and responsible for accelerating the folding and unfolding events [89].

QM/MM techniques have also been used to address solvation effects (partly in collaboration with E. Sánchez-García and other RESOLV partners). A combined experimental and theoretical study of diphenylcarbene showed that the spin state of such reactive carbenes can be controlled by halogen bonding (in this case with CF_3I and CF_3Br); on the theoretical side, DFT and ab initio calculations were performed to obtain gas-phase singlet and triplet potential energy surfaces for the corresponding complexes, while DFT/MM simulations were carried out at low temperatures (3 to 75 K) to check for the interconversion of these complexes in an argon matrix under these conditions [67]. A second joint study combined femtosecond transient absorption spectroscopy and QM/MM simulations to investigate two competing pathways for the reaction between singlet diphenylcarbene and methanol (O-H insertion) in methanol/acetonitrile solvent mixtures; the choice between the two pathways was found to be governed by the hydrogen bonding dynamics, with the key role being played not be the nearest solvent molecule but by its neighbor, which is the decision-maker rather than a spectator [70]. Solvent effects also turned out to be important in an ab initio QM/MM investigation of 4-thiothymidine in aqueous solution, which identified the intersystem crossings and the photophysical pathways that enable this molecule to act as a photosensitizer in photodynamic therapy [3]. Finally, the hydrophobicity of different solvents can be assessed experimentally and theoretically by determining the distribution coefficients of compounds between two solvent phases. In the context of the SAMPL5 challenge, we computed these quantities for the SAMPL5 target molecules using MM and QM/MM free energy simulations of water-cyclohexane transfer; both the BLYP/MM and the OM2/MM results turned out to be superior to the pure MM results [71].

Classical MD simulations are an integral part of all our QM/MM studies because they are indispensible for the setup of the system and for generating starting points for QM/MM calculations. In many cases, they also provide chemically relevant information, and they may even be sufficient to solve a given problem. We close this section by briefly mentioning two such examples (collaborative work with B. R. Crane). Classical and replica-exchange MD simulations show that changes in active-site histidine hydrogen bonding trigger the activation of cryptochrome, the principal light sensor of the insect circadian clock; more specifically, the photosensory mechanism of the cryptochrome from *Drosophila melanogaster* involves flavin photoreduction coupled to protonation of His378, whose altered hydrogen-bonding pattern leads to a conformational change in a key regulatory element of the protein (the C-terminal tail helix and its surroundings) [63]. In analogous MD simulations of the blue-sensing LOV (light-oxygen-voltage) protein Vivid, a Gln182 amide flip was found to occur in response to either adduct formation or reduction of the isoalloxazine ring to the neutral

semiquinone; this flip elicits long-distance allosteric responses in the protein that are crucial for signal transduction (manuscript submitted).

The ChemShell software that has been used in our QM/MM applications is available under a license agreement (see www.chemshell.org).

Publications resulting from this research area: 2, 3, 16, 18, 20, 23, 25, 32, 36, 39, 40, 42, 49, 61, 63, 64, 67, 70, 71, 83-85, 89

External funding: Cluster of Excellence RESOLV (DFG), SusChemSys (NRW)

Cooperations: M. Barbatti (Mülheim/Ruhr, DE); B. R. Brooks (NIH Rockville, USA); B. R. Crane (Cornell, USA); M. Elstner (Karlsruhe, DE); W.-H. Fang (Beijing, CN); A. V. Nemukhin (Moscow, RU); P. Nuernberger (Bochum, DE); E. Sánchez-García (Mülheim/Ruhr, DE); W. Sander (Bochum, DE); S. Shaik (Jerusalem, IL)

2.5.5 Research Area "Photoinduced processes in organic molecules" (M. Barbatti)

Involved: L. Stojanović, G. Pereira Rodrigues, D. Mancini, R. Crespo-Otero, W. Arbelo-González

Objective: After UV photoexcitation, organic molecules relax through a manifold of excited states, dissipating the absorbed energy either by photoemission or by vibrational excitation. The objectives of this research area are 1) to characterize these relaxation mechanisms through excited-state computational simulations; and 2) to implement new methods and algorithms to improve these simulations.

Results:

a) Fundamental processes

Photoexcitation may induce electron and proton transfers within the molecule or between neighbor molecules. We have investigated several cases to understand how this transfer process occurs, how it is triggered, and on which time scale it proceeds [93, 95, 96, 103].

In collaboration with E. Sánchez-García and W. Sander, we investigated the formation of weakly bound dimers of N-methylformamide (NMF) and their photochemistry after UV irradiation [95]. The aim was to understand the effect of UV radiation on peptide bonds. Starting from trans(donor)-trans(acceptor) dimers, the experiments carried out in the Sander group showed that the main products formed upon irradiation are the trans(donor)-cis(acceptor) dimers. Moreover, in contrast to the photochemistry of the NMF monomers, no dissociative products were observed upon 248 nm irradiation of the NMF dimers. On the basis of nonadiabatic dynamics simulations, we could explain the absence of dissociative products. The simulations showed that the NMF dimers are protected by a proton-transfer mechanism in the excited state that is faster than the photodissociation.

In another case study, I showed that an electron transfer from solvent molecules to the photoexcited chromophore can also induce internal conversion with little geometric distortion [93]. Using dynamics simulations, I found out that when a specific tautomer of adenine (7H-adenine) in water absorbs UV radiation, it dissipates the photo-energy as heat after receiving an electron from a nearby water molecule. This result revealed an

unknown internal conversion pathway, with implications for the assignment of photoreactions in biological environments and for the design of organic photodevices.

In a recent case study, we addressed the double proton transfer in 7-azaindole (7AI) dimers [103]. Two decades ago, A. Zewail and his team, using time-resolved spectroscopy, proposed that photoinduced double proton transfer in 7AI dimer is a stepwise process. Since then, this conclusion has motivated an uncommonly fierce debate on the nature of this transfer – whether it is really stepwise or alternatively concerted. Using high-level computational simulations of static and dynamic properties, R. Crespo-Otero, N. Kungwan, and I found out that much of these earlier discussions were induced by inappropriate theoretical modeling, which led to a biased interpretation of the experimental results. We showed that earlier models provided either a wrong or incomplete topographic description of the excited-state potential energy surface of the 7AI dimer. They delivered an inadequate balance between the energies of the local-excitation and charge-transfer regions, and completely missed the possibility of internal conversion to the ground state (Figure 12). We concluded that stepwise transfer is thermodynamically and kinetically disfavored and only concerted transfer takes place.

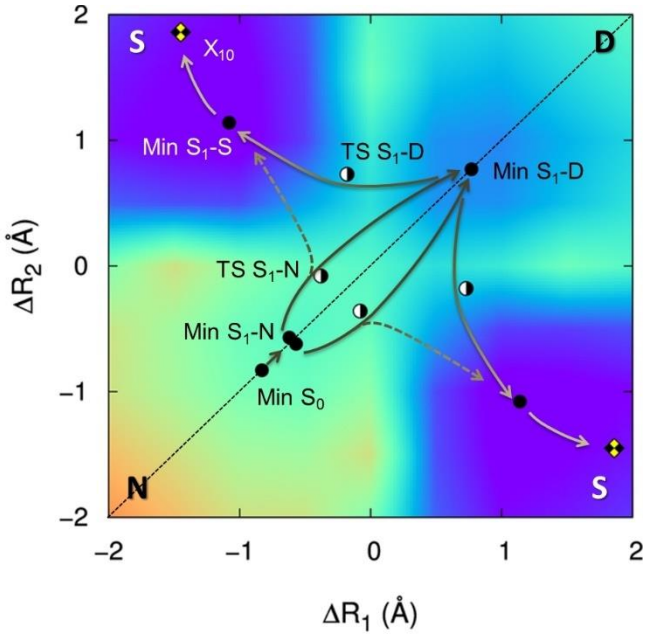

Fig. 12. Potential energy surface of the first excited state of the 7AI dimer. The presence of a conical intersection (X_{10}) blocks the occurrence of stepwise double proton transfer.

b) Applied photophysics

Photophysical and photochemical processes are core phenomena in diverse aspects of life on Earth. In the 2014-2016 period, we continued a long-term research program addressing such processes from a computational standpoint [13, 19, 31, 42, 62, 91, 94, 97, 100-102, 104, 107].

In collaboration with W. Thiel and T. C. Ramalho, we showed that excited-state proton transfer may give rise to new diagnostic tools to follow the clinical evolution of cancer patients [42]. It is well-known that a number of phenylbenzothiazole (PBT) compounds exhibit antitumor activity. Certain PBTs are also well-known for their very large Stokes shifts caused by excited-state intramolecular proton transfer (ESIPT). Aiming at connecting tumor selectivity and proton-transfer properties, we have theoretically designed and studied a new PBT compound, named HABT. Our hypothesis, confirmed by the simulations, is that the proportion and intensity of violet and green emissions from HABT depend on the protein active-site conformation, which modulates the rates of proton transfer, and of radiative and nonradiative decays. Thus, changes in the fluorescence spectrum of HABT bound to tyrosine kinases could be the basis for a new method to detect mutations in cancer cells, usually associated to development of drug resistance.

Still in the health field, I have completed a comprehensive map of processes that produce or cleave pyrimidine dimers (Figure 13) [94]. Cyclobutane pyrimidine dimers (CPD) are closely related to mutagenesis and carcinogenesis; they are formed when UV radiation induces dimerization of adjacent pyrimidine nucleobases. To understand how the dimerization and the repair process happen, I built a benchmark of computational results based on different methods. For these simulations, I used a thymidine-dimer model in the gas phase and explored the ground- and excited-state potential energy surfaces of neutral (singlet and triplet), cationic, and anionic species. The analysis of these surfaces allowed me to describe several reaction pathways for dimerization and repair, some of them completely unknown so far.

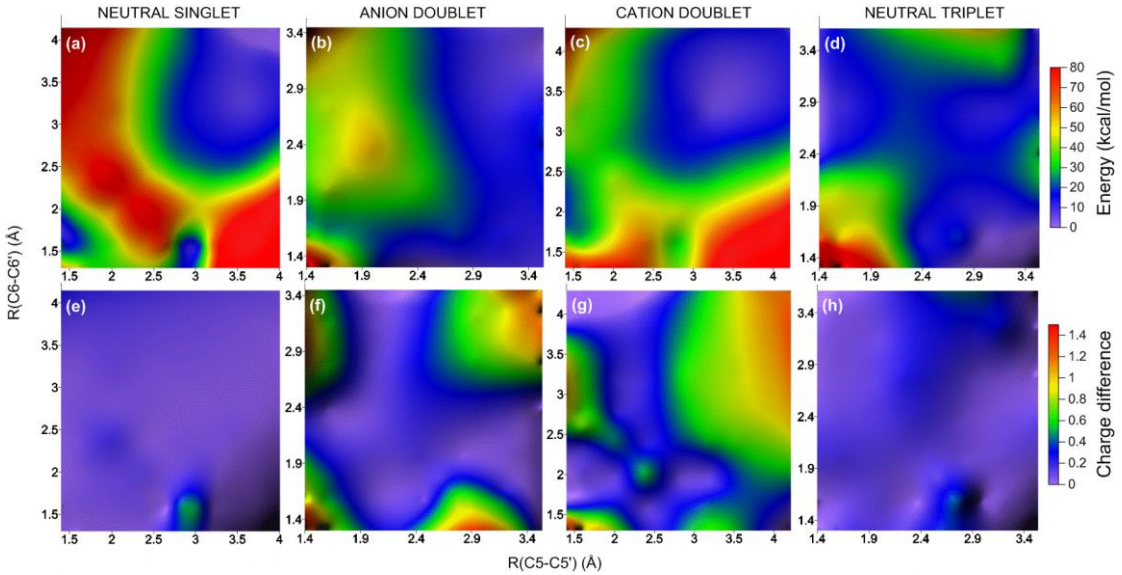

Fig. 13. Potential energy surface and charge distribution in the ground state of neutral and charged thymine dimers.

In collaboration with S. do Monte and R. Hilal, I have investigated the photochemistry of a series of halogen compounds, whose photoproducts may impact atmospheric chemistry [97, 104, 107]. One example is HCFC-132b (CF_2ClCH_2Cl), which is the major compound used for replacing CFC-113 ($CF_2ClCFCl_2$) in different industrial applications [107]. These simulations revealed how the radiation from different UV-wavelength regions interacts with these compounds and leads to formation of diverse products.

In recent years, the research on organic photovoltaics has become central in the field of photochemistry due to its high technological potential. Between 2014 and 2016, we investigated the fundamental properties of diverse organic compounds of interest for photoenergy conversion [13, 19, 31, 62, 102], including oligothiophenes (collaboration with W. Thiel) [31, 62], squaraine-fullerene complexes (also with W. Thiel) [19], and poly-(p-phenylene vinylene) (PPV) oligomers (with H. Lischka) [102]. In all these studies, our focus was the development of analytical tools to characterize charge and energy transport processes. In the case of oligothiophenes, for instance, we developed a new computational approach, in which the energy, relative ordering, and population of productive and unproductive electronic states of a molecular aggregate are monitored during the dynamic relaxation following photoexcitation. Applying this approach to a particular system – the photoexcited bi-thiophene dimer – we showed that few femtoseconds after light absorption, the dimer has two electronic energy bands separated by a sizable energy gap [62]. The high-energy band has a productive state lying on its bottom, while the low-energy band is composed of unproductive states only.

As the dimer relaxes, it populates the productive state on the bottom of the high-energy band. If the gap separating the bands remained constant, this productive state would survive for a long time, contributing to current generation. However, induced by molecular vibrations, the energy gap fluctuates and, when it gets to a minimum, the population is transferred to the low-energy unproductive band. As a result, the productive state survives for not more than 100 fs, rendering poor power conversion performance.

c) Method and program development

Since 2005, we have been designing and developing the Newton-X platform [92]. Newton-X is a collection of programs to perform all steps of excited-state nonadiabatic dynamics simulations, from the generation of initial conditions to the statistical analysis. The project involves collaborations with H. Lischka, J. Pittner, and others. Newton-X is an open-source platform distributed free of charge. Between 2014 and 2016, we finished the development of new interfaces for nonadiabatic dynamics using different wavefunctions and codes: MCSCF / GAMESS (collaboration with T. Windus) [99]; CC2 and ADC(2) / Turbomole; and (U)TDDFT, (U)TDA, and (U)CIS / Gaussian 09 [98, 106].

We have additionally implemented a new method for simulating steady and time-resolved photoelectron spectra based on nuclear ensembles (Figure 14) [105].

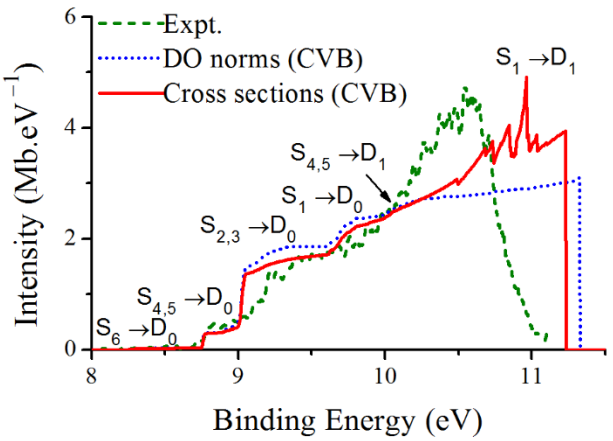

Fig. 14. Simulated time-resolved (0-25 fs) photoelectron spectrum of imidazole compared to experimental results.

Future directions: I was appointed professor of the chair of excellence A*MIDEX at the University Aix-Marseille, where I am since September 2015. A productive

collaboration with W. Thiel's group is still in place. We have been working on the characterization of exciton formation in an ensemble of organic heterojunctions for organic photovoltaics (collaboration with D. Fazzi) and on the development of a new program for computing spin-orbit couplings based on DFT methods (collaboration with X. Gao).

Outreach: Access to the Newton-X platform is gained via the Newton-X webpage (www.newtonx.org), where a full documentation and tutorials are available.

Publications resulting from this research area: 13, 19, 31, 42, 62, 91-107

External funding: DAAD DE/BR; KAU (SA); DAAD DE/HR; A*MIDEX (FR)

Cooperations: I. Antol (Zagreb, HR); A. C. Borin (Sao Paulo, BR): R. Crespo-Otero (London, UK); H. Hilal (Jeddah, SA); N. Kungwan (Chiang Mai, TH); H. Lischka (Lubbock, USA); T. C. Ramalho (Lavras, BR); E. Sánchez-García (Mülheim, DE); W. Sander (Bochum, DE); W. Thiel (Mülheim, DE); S. Ullrich (Athens, USA); O. Weingart (Düsseldorf, DE); T. Windus (Ames, USA)

2.5.6 Research Area "Molecular interactions in organic and biological systems. Applications and methodological implementations" (E. Sánchez-García)

Involved: K. Bravo-Rodriguez, S. Mittal, P. Sokkar, N. Tötsch, J. Iglesias, M. Fernandez-Oliva, S. Carmignani, G. Gerogiokas, V. Muñoz Robles, J. Mieres, L.Wollny

Objectives: In the Sánchez-García group, molecular interactions are used as a tool to tune the properties of chemical and biological systems. In this context three very much interconnected, general lines are developed (Figure 15). One key topic is the study of ***molecular interactions in biological systems,*** namely protein–ligand interactions, protein–protein interactions, enzymatic activity, and computational mutagenesis, as well as the effect of solvent on these processes. Another research line is the study of ***molecular interactions in chemical reactivity***, where we focus on reactive intermediates and unusual molecules and the effect of molecular interactions on their stability, spectroscopic properties, and reactivity. At the core of these applications lies the use and methodological implementation of ***multi-scale computational approaches***.

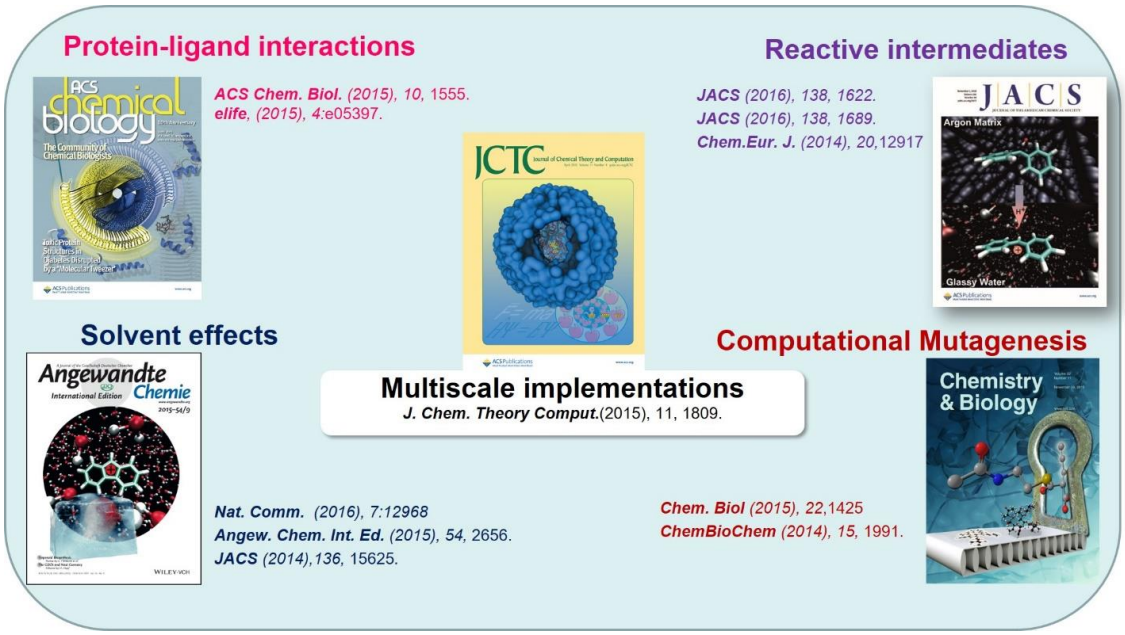

Fig. 15. Main research lines and selected representative publications of the Sánchez-García group in 2014-2016.

Results:

Molecular interactions in biological systems

a) Protein-ligand interactions

Interactions with small molecules can significantly influence the functionality of systems of diverse structural complexity – from amyloidogenic peptides to large proteins and enzymes. In our group we develop computational models of protein-ligand complexes to study their association and how such molecules can modulate protein–protein interactions. The combination of molecular dynamics simulations with free energy calculations and QM/MM methods allows us to predict ligand binding sites in a protein and to identify interactions patterns for an *in silico* design of improved ligands able to reach specific protein regions of biological relevance.

Specifically, we investigate the effect of selective ligands such as molecular tweezers (MT) that bind specifically to lysine and arginine residues, and molecules with a guanidiniocarbonylpyrrole (GCP) moiety targeting negatively charged amino acids. We are also interested in less specific compounds like aromatic heterocyclic derivatives and peptide ligands.

CLR01 is a lysine- and arginine-specific hydrogen phosphate tweezer able to inhibit the self-assembly and toxicity of several amyloid proteins *in vitro* and *in vivo*. In this context, we studied the interactions of the islet amyloid polypeptide (IAPP) with CLR01. Here, the selective binding to critical lysine residues is the molecular basis for the effect of the tweezer that causes IAPP to adopt an off-pathway conformation not found in the absence of CLR01 [117].

$PAP_{248\text{-}286}$ is the prototype amyloidogenic peptide in semen, closely related to the transmission of HIV-1. We found that CLR01 is able to bind all positively charged residues of $PAP_{248\text{-}286}$ in a conserved manner. Conversely, a control molecule consisting of the charged core of CLR01 only features labile interaction patterns with $PAP_{248\text{-}286}$. Thus, we were able to explain the lack of experimental effect of the spacer vs. the inhibition of toxicity by the tweezer [118]. Notably, the experimental studies indicated that CLR01 has a dual activity, namely destroying diverse enveloped viruses (including HIV) and remodeling amyloid fibrils in semen. To clarify how CLR01 can exhibit these two distinct activities, we also studied the molecular tweezer CLR05 that acts as potent anti-viral activity agent with no anti-amyloid activity. Unlike CLR01, the substituents in CLR05 are methylene carboxylate groups. Our previous studies with single amino acids and small peptides indicated that the hydrogen phosphate tweezer CLR01 threads lysine

or arginine side chains very efficiently through its tweezer cavity, while the carboxylate derivative CLR05 is only able to weakly bind the free amino acid outside its cavity by simple ion pairing. Hence, by investigating the CLR05 interaction with $PAP_{248-286}$ we could show that CLR05 is less able to form inclusion complexes with lysine or arginine compared to CLR01. The global minima on the peptide-tweezer free energy surfaces obtained from adaptive biasing force calculations indicated that binding of CLR05 to residues at the N- and C-terminal regions of $PAP_{248-286}$ is not favored. In addition, free energy perturbation calculations predicted that, in $PAP_{248-286}$, CLR01 forms better inclusion complexes than CLR05 for almost all Lys/Arg residues. Thus, we proposed that CLR05 may lack the anti-amyloid activity displayed by CLR01, in agreement with the experimental results (manuscript submitted).

We also studied the interactions of CLR01 with the Huntingtin protein exon-1. This protein is a key target in therapeutic strategies against Huntington's disease (HD), a neurodegenerative disorder without cure. We showed that the lysine residues found at low concentration in the N-terminal fragment of the exon-1 sequence (N17) are crucial for htt aggregation since binding of CLR01 induces structural rearrangements within the htt exon-1 monomer. In a joint experimental and computational study, we also demonstrated that CLR01 potently inhibits htt exon-1 aggregation, underpinning the key role of N17 in modulating htt exon-1 toxicity (manuscript submitted).

We previously reported studies on the selectivity of CLR01 towards Lys residues in a 14-3-3 protein. Now, we wanted to investigate also Arg complexation by molecular tweezers on proteins. In a combined experimental (P. Bayer, Essen) and computational study, we revealed the affinity profile of the tweezers to preferred lysine and arginine residues on the surface of the N-terminus region of the p97 protein (p97-N). Our QM/MM calculations confirmed the preferred complexation sites but also allowed us to discriminate between ambiguous host residues derived from NMR data. The binding of the tweezer to p97-N resulted in the inhibition of the protein-protein interaction between p97 and its cofactor UBXD1 [123].

In another multidisciplinary study using protein crystallography, biophysical affinity determination, and biomolecular simulations, we revealed the structural details of how the molecular tweezer CLR01 influences the 14-3-3/Cdc25CpS216 protein-protein interaction (PPI). CLR01 acts as a supramolecular "Janus" ligand that can bind simultaneously to a flexible peptidic PPI recognition motif and to a well-structured adapter protein (Figure 16). This binding "freezes" one of the conformational states of

the intrinsically disordered Cdc25C protein partner and enhances the apparent affinity of the interaction (manuscript submitted).

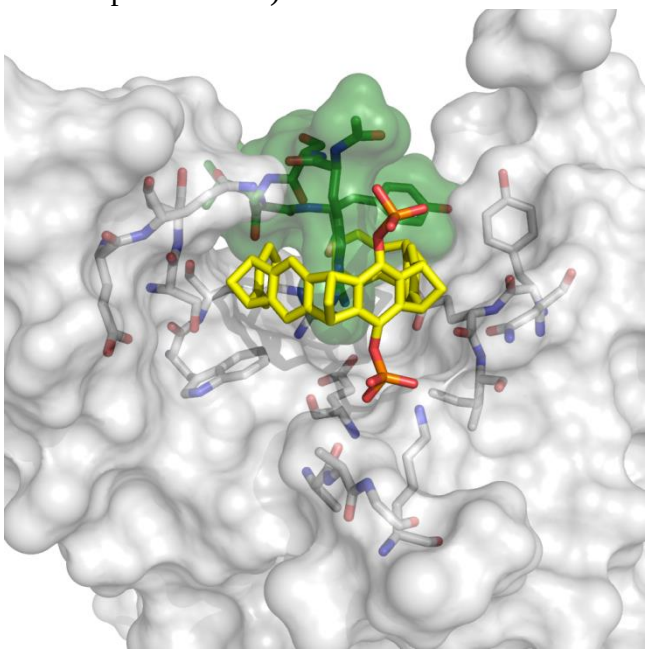

Fig. 16. CLR01 traps Arg 208 of Cdc25C (green surface) inside its cavity and simultaneously establishes contacts with 14-3-3ζ (white surface) via its hydrophobic sidewalls (yellow).

In another study on the 14-3-3ζ protein, we presented the first example of a small molecule binding to the 14-3-3ζ dimerization interface. This compound, featuring a GCP motif, was designed by rational *in silico* optimization of a peptidic ligand identified from a biochemical screening of a peptidic library. The binding was characterized by UV/Vis, MST, multiscale simulations, and X-ray crystallography. QM/MM MD simulations allowed us to investigate the binding of the ligand in solution and confirmed the dimer interface as preferred binding site (manuscript submitted).

The ribosome is a highly relevant but also complex system for ligand design. Macrolides, which are commonly used as antibiotics, are ligands targeting the ribosome. They can selectively bind at the prokaryote ribosome, inhibiting its function. Due to the increased antibiotic resistance of pathogenic strains, there is high interest in designing new synthetic macrolide molecules with enhanced binding to the ribosome. We used molecular dynamics simulations, free energy calculations, and QM/MM methods to study the binding of antibiotic derivatives to the ribosome in explicit solvent. This allowed us to establish which modifications of the macrolide core result in binders with better affinity and to clarify the role of the hydration free energy and conformational entropy on the binding events (unpublished work).

b) Protein-protein interactions and computational mutagenesis

Polyketides are natural products frequently used for the treatment of various diseases, but their structural complexity hinders efficient derivatization. In this context, we introduced enzyme-directed mutasynthesis to incorporate non-native extender units into the biosynthesis of erythromycin. More recently, we extended the molecular rationalization of enzyme-substrate interactions through modeling, to investigate the incorporation of substrates with different degrees of saturation of the malonic acid side chain. This allowed the biosynthesis of new erythromycin derivatives and the introduction of additional mutations into the AT domain for a further shift of the enzyme's substrate scope [113].

We are also interested in the study of disease-causing mutations in complex systems like *high temperature requirement A* (HTRA) serine proteases. Our free energy perturbation calculations predicted which of such mutations strongly destabilize the HTRA1 trimer. Molecular dynamics simulations of the wild type HTRA1 and the mutated systems allowed us to identify key interactions for the integrity of the enzyme. Our data suggested the presence of an intricate network of interactions composed of a hydrophobic cluster and two salt bridges that mediate trimer formation in this enzyme (unpublished work).

In addition to the human HTRA1, we also studied the bacterial serine protease DegP, this time as protein guest in a DNA origami host. Two models were considered for the binding of the 24-mer of DegP ($DegP_{24}$) inside the origami cage. In one model, $DegP_{24}$ interacts with opposite sides of the hexagonal cage while in the second model $DegP_{24}$ interacts with consecutive sides of the hexagonal cage. For each setup two binding motifs were considered. Our atomistic geometric models along with MD simulations suggested that the presence of three ligands per origami face should provide the maximal probability for binding to occur and that all DegP forms, although with distinct space-filling capabilities, can be hosted inside the DNA prisma (manuscript accepted, Nature Communications).

CXCR4 is a receptor protein of the chemokine receptor family. The CXCR4/CXCL12 signaling pair is associated with a variety of diseases like cancer cell metastasis or chronic inflammation. EPI-X4 is a peptide that specifically interacts with the receptor, thereby blocking CXCR4 (X4)-tropic HIV-1 infection and CXCL12 signaling. Our computational studies allowed us to propose binding sites of the peptide on CXCR4. The molecular environment was explicitly considered by embedding the protein in a full

atomistic membrane model and explicit water molecules. Our work revealed which residues of EPI-X4 are essential for receptor binding. On this basis, we made specific predictions for a next generation of EPI-X4 derivatives with improved binding efficiencies. These predictions were experimentally proven by the group of J. Münch (Ulm) and resulted in the generation of even more potent leads (unpublished work).

Molecular interactions on chemical reactivity

Carbenes and carbenium ions are challenging molecules and among the most important reactive intermediates in chemistry. They play key roles in a large number of reactions. In nucleophilic solvents such as alcohols, they can be extremely short-lived (lifetimes in the order of picoseconds), and it was believed that the corresponding cations could be stabilized only in super-acidic, non-nucleophilic solvents. We recently used QM MD and QM/MM MD approaches to investigate the reaction of diphenylcarbene (DPC), an archetypical triplet state carbene, with water in argon matrices and in water ice at 3 K. The combined matrix isolation (W. Sander, Bochum) and computational study allowed us to establish that, in the complex with a single water molecule, the triplet ground state of DPC is switched to its singlet state, stabilized by a strong hydrogen bond with water [109]. A similar effect was found for fluorenylidene (FY), where we also demonstrated that hydrogen bonds with protic solvents like water strongly influence the reactivity of the carbene by selectively stabilizing the singlet state and thus inverting the singlet-triplet gap [114].

The interactions between DPC and the halogen bond donor CF_3I were studied using QM and QM/MM calculations. CF_3I forms very strong complexes with the singlet state of DPC, but interacts only weakly with triplet DPC. This results in a switching of the spin state of DPC, with the singlet complex becoming more stable than the triplet complex. CF_3I forms a second complex (type II) with DPC that is thermodynamically slightly more stable. Our calculations predicted that in this second complex the DPC···I distance is shorter than the F_3C···I distance, whereas in the first complex (type I) the DPC···I distance is, as expected, larger. The type II complex could be only found as a minimum in the matrix environment (QM/MM calculations) and the interconversion was temperature-dependent. We also performed a 2-dimensional potential energy scan with the halogen bond distance and angle as reaction coordinates to explore the relative stability of these structures. The type II complex is characterized by a C-I distance of 2.3 Å. It is stable over a range of C-I-C angles while the type I structure is characterized by a nearly linear C-I-C angle and is stable over a range of C-I distances. Our study of intersystem crossing in the reaction of DPC and CF_3I indicated that it may occur when

the C-I distance is between 3.25 and 3.90 Å. The large calculated spin-orbit coupling may facilitate the intersystem crossing [67].

Unlike DPC and FY, bis(*p*-methoxyphenyl)carbene is the first carbene to be isolated in both its lowest-energy singlet and triplet states. We studied the influence of the C-C-C bond angle at the carbene center and of the conformational flexibility of the methoxy groups on the singlet-triplet gap. Unlike the carbene angle, the orientation and rotation of the methoxy groups have basically no influence on the relative stability of the conformers in the singlet or triplet state. In addition, to assess the impact of water on the singlet-triplet gap, several water complexes were computed considering not only the carbene center as a potential H-bond acceptor, but also both oxygen atoms of the methoxy groups. We found that hydrogen bonding with the methoxy groups shows a small tendency to stabilize triplet states over singlets, which is however not pronounced enough to overcome the larger effect of the interaction of water with the carbene center that strongly stabilizes the singlet [122].

In addition to the interactions with water, we were also interested in the effect of organic solvents and their mixtures on singlet-triplet gaps and carbene reactivity. In a combined broadband femtosecond transient absorption (P. Nürnberger, Bochum) and QM/MM study, we showed that for DPC the decision-maker is not the nearest solvent molecule but its neighbor. Therefore, variation of the solvent mixing ratio allows control over the reactivity of DPC. Using QM/MM molecular dynamics simulations, we also proposed two mechanisms for OH insertion into DPC by methanol [70] (Figure 17) and predicted possible side reactions.

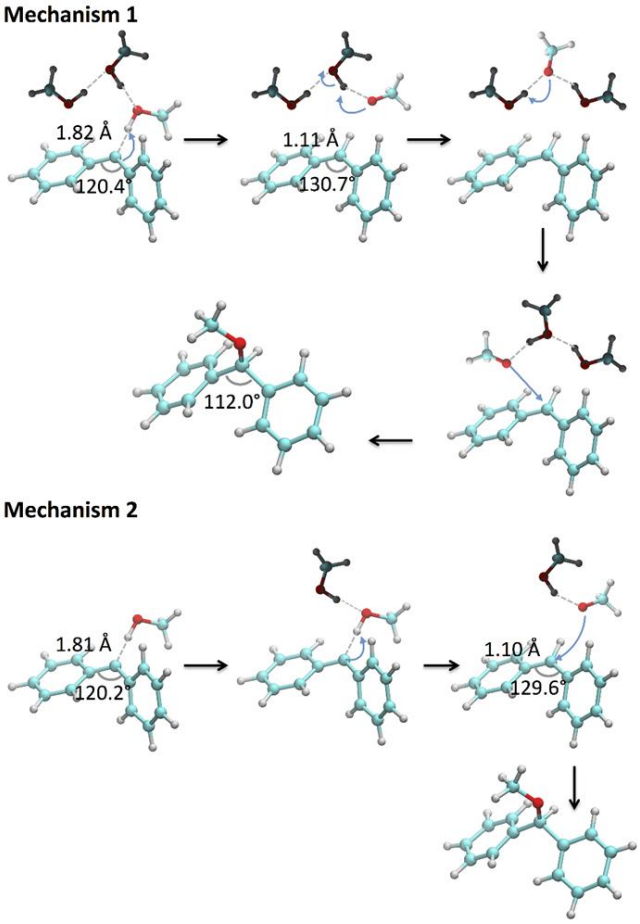

Fig. 17. Mechanisms 1 and 2 of O-H insertion for the reaction of singlet DPC with methanol, as observed in the QM/MM MD simulations. Average distances and angles are given.

Multi-scale computational approaches

Hybrid methods are at the core of our research. ChemShell is a QM/MM modular package that allows the combination of several QM and MM methods. Currently, there is considerable interest in the development of coarse-grained (CG) force fields to improve the performance and sampling in MD simulations and geometry optimizations. Although the CG methodology has been successfully applied to very large molecular systems, it does not allow the study of fine structural details due to the approximate CG representation. In this context, we have implemented a QM/MM/CG protocol in ChemShell. This approach was validated using two enzymes: chorismate mutase (CM) and p-hydroxybenzoate hydroxylase (PHBH). We also evaluated the role of CG modeling on biocatalysis. In CM, the inclusion of an atomistic MM water layer was necessary for a correct description of the energy profile. In the case of PHBH, the use of the polarizable CG model for the outer water did not affect the stabilization of the highly charged FADHOOH-pOHB transition state compared to the fully atomistic QM/MM calculations. A detailed performance analysis in a glycine−water model

system indicated that computation times for QM energy and gradient evaluations at the density functional level are typically reduced by 40−70 % for QM/MM/CG relative to fully atomistic QM/MM calculations [49].

We are currently working on the implementation of an interface to GROMACS in ChemShell and on the implementation of grid cell theory at the multiscale level. We are also implementing an approach to explore potential energy surfaces and to find thermally allowed intersystem crossings (ISC) in reactive intermediates based on QM molecular dynamics simulations.

Future directions: I plan to continue working on protein-ligand interactions. This will be extended to molecular tweezers with specific binding anchors designed to target certain regions of interest in the protein. Multivalent guanidiniocarbonylpyrrole ligands and novel peptide derivatives will also be investigated. The influence of the solvent on protein-protein interactions, enzymatic activity, and catalysis will be in the focus of our research. New reactive intermediates and their interactions with other organic molecules will be explored, and our QM MD approach for ISC will be implemented at the multiscale level to account for solvent and environmental effects.

Publications resulting from this research area: 49, 67, 70, 95, 108-123

External funding: Chemical Industry Funds (Liebig Stipend), German Research Foundation: RESOLV Cluster of Excellence (EXC 1069), Collaborative Research Center “Supramolecular Chemistry on Proteins” (SFB 1093), Boehringer Ingelheim Foundation (Plus-3 grant)

Cooperations:; P. Bayer (Essen, DE); G. Bitan (Los Angeles, US); R. Crespo-Otero (London, U.K); S. Ebbinghaus (Bochum, DE); M. Ehrmann (Essen, DE); J. Münch (Ulm, DE); P. Nürnberger (Bochum, DE); C. Ottmann (Eindhoven, NL); B. Sacca (Essen, DE); W. Sander (Bochum, DE); F. Schulz (Bochum, DE); T. Schrader (Essen, DE); W. Thiel (Mülheim/Ruhr, DE); E. Wanker (Berlin, DE)

2.5.7 Research Area "Biomolecular Solvation" (M. Heyden)

Involved: R. Persson, C. Päslack, V. Pattni, Y. Xu, B. Majumdar, A. Singh, D. Ray

Objective: Fundamental biomolecular processes involve major changes of the solvation for the involved molecular species: aggregation, folding, unfolding or conformational changes of proteins, complex formation of enzymes with their substrates, and the binding of ligand or drug molecules to receptors. Consequently, solvation free energies are a major driving force that determines thermodynamic equilibrium as well as kinetic barriers. Here, we develop novel simulation and analysis procedures to study microscopic contributions to the solvation free energy, which can be utilized for enzyme and drug design, as well as to understand a particular biomolecular system. Further, we utilize this information to improve implicit solvent simulations of concentrated biomolecular solutions on the *meso*-scale, which can describe realistic *in vivo* environments of biochemical processes.

Results: Atomistic molecular dynamics simulations with explicit solvent molecules contain, in principle, all the information required to analyze the influence of a molecular solute on the solvent energetics and structure. However, extracting this information, in particular separating energetic and entropic contributions to the total free energy, is often a challenging task. We have now developed a novel technique (3D-2PT), which provides not only total solvation energies and entropies of a given molecule, but resolves their local contributions in the three-dimensional environment of a molecule. A main challenge is the spatial resolution of the local solvent entropy, which we obtain from analyzing the local vibrational density of states (VDoS) of the solvent. The latter is obtained from time-dependent fluctuations of atomic velocities. Figure 18 shows an example analysis for a small model solute, which exhibits the chemical features of a peptide bond. Of particular importance for the analysis are low-frequency modes in the

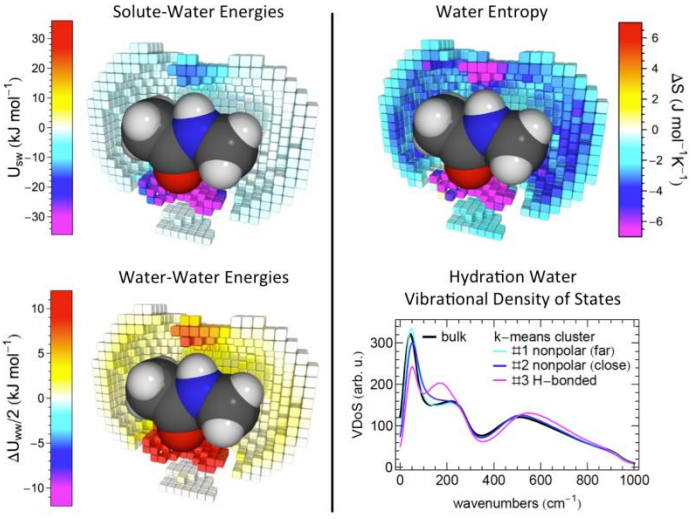

Fig. 18. Solvation free energy contributions in the hydration shell of N-methylacetamide. Local hydration water entropies are derived from spectra of thermally excited intermolecular vibrations (bottom right).

far-infrared range (0-330 cm^{-1} or 0-10 THz) of the vibrational spectrum, which are primarily characterized by intermolecular vibrations in the solvent, e.g. vibrations of the water hydrogen bond network. These vibrations are thermally accessible (k_BT/h=6 THz at 300K) and therefore carry the main part of the entropic information (Figure 19). The method can be applied for simulations of large biomolecular systems containing ~100,000 of atoms (Figure 20) and non-aqueous solvents.

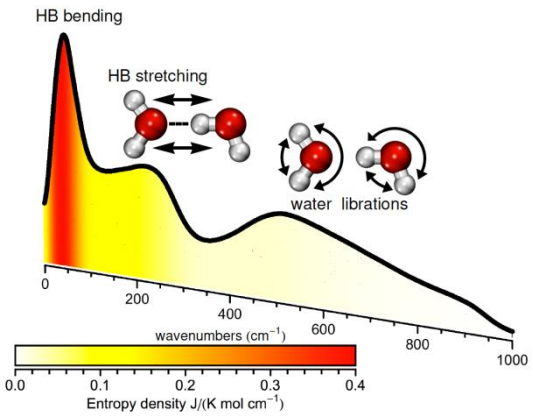

Fig. 19. Entropy information of characteristic intermolecular vibrations in the vibrational density of states of water.

A thermodynamic analysis based on the spectrum of intermolecular vibrations is particularly powerful in combination with spectroscopy experiments, which can follow changes in the solvent spectrum. This is realized by our cooperation partner Martina Havenith at the Ruhr-University Bochum, who develops time-resolved terahertz absorption spectroscopy methods. This technique allows for studies of non-equilibrium processes during a triggered reaction on a millisecond timescale, i.e. enzymatic catalysis in a stopped-flow experiment and protein unfolding/refolding after a laser-induced T-jump. Here, simulations of the biomolecular systems at different stages of the process can reproduce the observed spectral changes, in particular shifts of vibrational frequencies, and provide the microscopic information for the interpretation in terms of changes in the solvation energy, entropy and free energy.

Our analysis of spatially resolved thermodynamic properties of water in the hydration shell of proteins further allows detailed studies of the complex and non-additive effects that govern the interactions of biomolecules with their solvent, as well as their binding partners, i.e. ligands, substrates, or potential drug molecules. Biomolecular surfaces feature a heterogeneous mix of functional groups as well as various convex and concave surface curvatures. Both, surface topology and the chemical nature of solvent-accessible groups affect the solubility of a protein interface and the binding of other molecules. This results in broad distributions of hydration water properties, i.e. binding energies and local entropies.

Equally broad distributions are observed for hydration water dynamics, i.e. hydrogen bond network fluctuations, rotational relaxation and translational diffusion. These dynamic processes can be characterized in simulations via time correlation functions,

which is a routine application in our lab. A combined analysis of local thermodynamic and dynamic properties of water in the hydration shell of proteins allows us to study fundamental correlations between both. In particular, we can demonstrate that the molecular entropy of water is related to translational and rotational dynamics. Studying these correlations in detail provides the key for the thermodynamic interpretation of experimental observables that are sensitive to local hydration water dynamics at various sites of a biomolecular surface. For example, Overhauser dynamic nuclear polarization (ODNP) can be used to study local hydration water mobility in the vicinity of spin-labels attached to selected sites in the protein. These experiments are carried out in the group of our partner Songi Han at UC Santa Barbara. Our simulations are able to reproduce the observed variations in hydration water mobility, while providing at the same time a semi-quantitative ruler to translate experimentally detectable variations of local dynamics into variations in entropy.

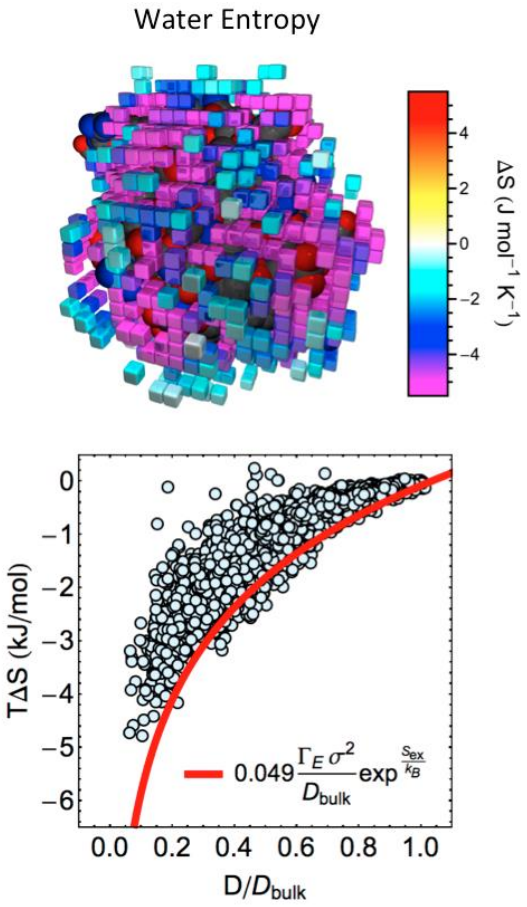

Fig. 20. Local hydration water entropies in the hydration shell of ubiquitin (top) are partially determined by local diffusion (bottom). The universal scaling law (red line), derived previously for bulk liquids, provides a lower limit for the local entropy (Dzugutov, M. *Nature* **1996**, *381*, 137-139).

A new target application of spatially resolved solvation free energies is their use as effective desolvation potentials in implicit solvent simulations of *meso*-scale systems of multiple interacting proteins and biomolecules. Together with the group of Douglas Tobias at UC Irvine, we recently developed a novel Monte Carlo simulation technique that includes efficient sampling of protein flexibility in simulations of complex protein solutions (Figure 21). We could show that this treatment significantly improves predictions of protein-protein interactions; however, the empirical treatment of (de)solvation free energies in the implicit solvation model remains a source of error. Our 3D-2PT approach enables us to derive tailored desolvation free energy potentials for the studied proteins directly from explicit solvent simulations, which then allow accurate simulations of biomolecular aggregation and molecular recognition in conditions resembling realistic biomolecular environments.

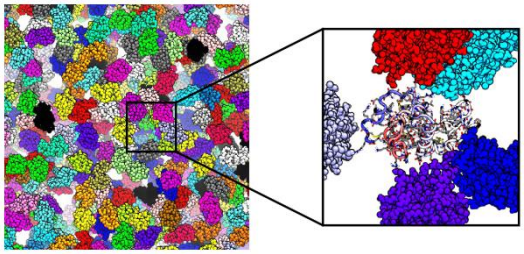

Fig. 21. Multiple-Conformation Monte Carlo simulation of a concentrated solution of lysozyme (169 mg/ml).

Future directions: We plan to extend the 3D-2PT methodology to mixed solvents, to develop a machine-learning procedure for the fast prediction of solvation free energies based on datasets generated by 3D-2PT simulations, and to derive computational tools to optimize the solvation free energy of lead compounds and ligand complexes.

Publications resulting from this research area: 124, 125, 128, 129, 132, 133, 134

External funding: Cluster of Excellence RESOLV (EXC-1069); European Research Council (via ERC Advanced Grant to M. Havenith); DAAD (stipend to D. Ray)

Cooperations: J. Dzubiella (Berlin, DE); S. Ebbinghaus (Bochum, DE); S. Han (Santa Barbara, US); M. Havenith (Bochum, DE); T. Head-Gordon (UC Berkeley, US); D. Russo (Grenoble, FR); L. Schäfer (Bochum, DE); D. J. Tobias (Irvine, US); M. Weik (Grenoble, FR)

2.5.8 Research Area "Ab Initio Quantum Chemical Methods for Complex Molecular Systems" (M. Roemelt)

Involved: A. Khedkar

Objective: A physically meaningful theoretical description of many complex molecular systems requires the usage of multireference methods. These methods treat a small part of the molecule, the so-called "active space", exactly while the rest of the molecule is subject to approximations. In the last decade mathematical techniques such as the Density Matrix Renormalization Group (DMRG) have emerged that allow for multireference calculations with active space sizes that are out of reach for comparable standard quantum chemical methods. The objective of this research area is to develop extensions to the DMRG Ansatz that improve its accuracy and to allow the calculation of magnetic properties. Furthermore, application of these methods to transition metal compounds aims at understanding their unique physical and chemical properties.

Results: In the last decade the ab initio density matrix renormalization group (DMRG) has been shown to provide a reasonable and accurate alternative to complete active space (CAS) methods as basis for molecular multireference calculations. It can be regarded as an approximation to the exact diagonalization of the large Hamiltonian matrix in the basis of many-electron wavefunctions within the active orbital space. A great advantage of DMRG is that it approximately solves a problem whose complexity scales exponentially with increasing system size by optimizing only a polynomial number of parameters. Owing to this favorable behavior DMRG is able to treat large active spaces on the order of 20-80 orbitals. However, quantitative accuracy is only reached if dynamic electron correlation effects are considered, too. In the reporting period we have developed a novel approach to the combination of DMRG and strongly contracted second-order N-electron valence perturbation theory (SC-NEVPT2) for quantum chemical multireference calculations [138]. The main objective of this approach is to lower the cost of treating systems with large active spaces and large orbital spaces with a moderate and controllable accuracy. The complexity of the problem and the computational cost are reduced by projecting the perturber functions as well as the unperturbed Hamiltonian onto a reduced Hilbert space. The form of this reduced space is determined by a modified density matrix renormalization procedure. This procedure ensures that both the electronic ground state and the perturber functions are accurately approximated during the calculation. As a result, the total energy (DMRG + SC-NEVPT2) converges rapidly and smoothly towards the exact value with

increasing number of states in the renormalized Hilbert space as demonstrated for a dimeric Cu cluster (cf. Figure 22).

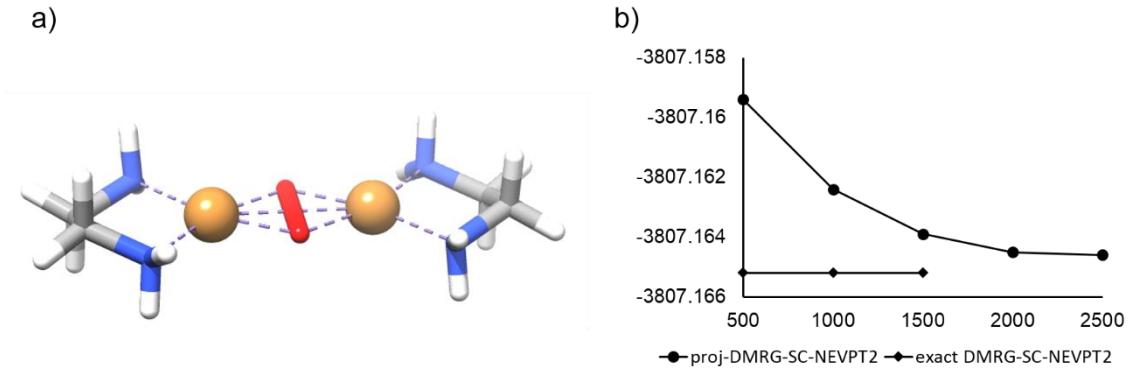

Fig. 22. Ball and stick visualization of $[Cu_2O_2(en)_2]^{2+}$ (a) and total energy calculated with the projected DMRG-NEVPT2 with respect to the bond dimension M (b).

Furthermore we have developed an approach to describe spin-orbit coupling (SOC) on top of a regular Born-Oppenheimer DMRG calculation in the framework of quasi-degenerate perturbation theory (QDPT) [136]. This approach accounts for SOC effects on the many-electron level and can thus be thought of as the molecular equivalent of atomic Russell-Saunders or LS coupling. With the spin-orbit coupled wavefunctions at hand the molecular g-tensors can be calculated in a rigorous and phenomenological way as proposed by Gerloch and McMeeking in 1975. Importantly, since the SOC matrix is fully diagonalized within a finite set of many-electron states, our approach is able to produce qualitatively and quantitatively correct results even for systems with a near-degenerate ground state. For example, the behavior of the molecular g-values of a Mo(III) trisamidoamine catalyst as it is distorted along its Jahn-Teller axis is correctly reproduced (cf. Figure 23). In contrast, regular linear-response type or single reference perturbation theory methods are bound to fail in these cases.

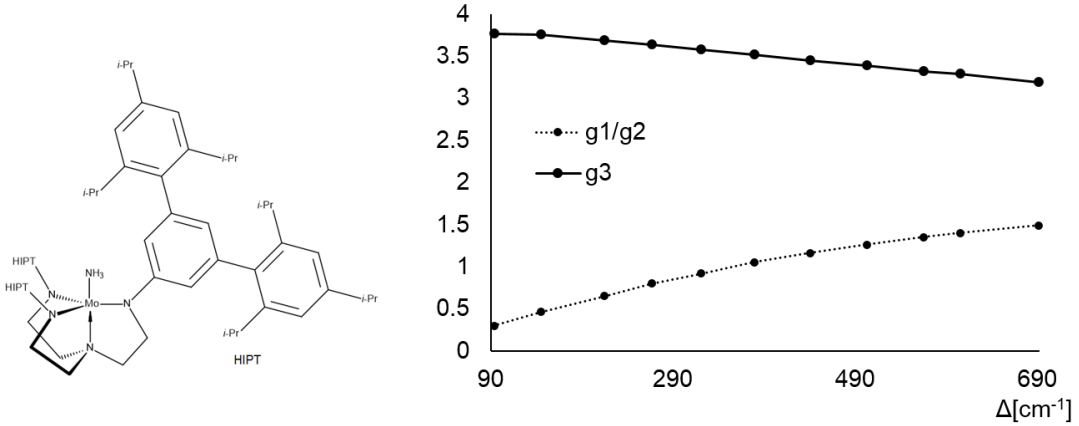

Fig. 23. Left: The chemically active Mo(III) trisamidoamine ammonia complex that is a crucial intermediate in the Yandulov/Schrock cycle. HIPT = hexaisopropylterphenyl. Right: The evolution of its molecular g-values with increasing Jahn-Teller splitting of the near-degenerate electronic ground state doublet.

During the reporting period our group has written our own standalone SCF and DMRG-SCF program from scratch. It has a variety of features including

- SCF for closed and open-shells
- DMRG-SCF (DIIS and full Newton Raphson)
- Density fitting
- Nuclear gradients
- Conventional and projected (vide supra) DMRG SC-NEVPT2
- Automated formula generation based on second quantization operator algebra
- Interfaces to the ORCA and PySCF program packages

The code is fully parallelized and utilizes the LibInt integral generation library by E. Valeev as well as the BLOCK code by G.K.-L. Chan. In the future it will be used in computational studies and moreover serve as basis for further developments in this field such as automated active orbital selection schemes and nonadiabatic coupling coefficients.

A study of the magnetic coupling constants of dimeric Mn compounds (cf. Figure 24), including a mixed-valence species, with DMRG-based methods elucidated the importance of different orbital subspaces for the description of magnetic coupling with *ab initio* techniques (manuscript in preparation). As anticipated, it could be shown that in addition to the Mn *3d* orbitals, the occupied *2p* orbitals of bridging oxo groups play an important qualitative role in magnetic coupling. In contrast, unoccupied oxo-orbitals or any orbitals that are located on bridging carboxylate groups contribute only in a minor way to the observed antiferromagnetic behavior. Moreover, the obtained results demonstrate that quantitative correct results can only be expected when dynamic electron correlation is explicitly taken into account.

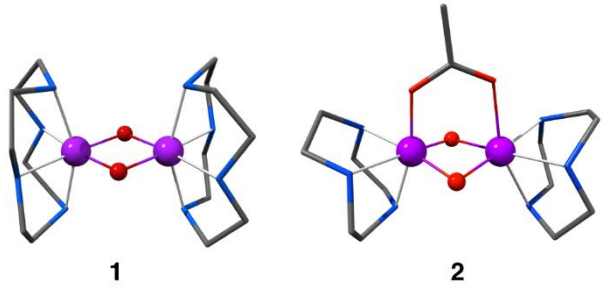

Fig. 24. Structures of the investigated Mn complexes. Color scheme: Mn purple, O red, N blue, C grey. Hydrogen atoms are omitted for clarity.

Future directions: Applications of the aforementioned theoretical methods will yield insight into the physical and chemical properties of complex molecular systems. A second scheme for the inclusion of SOC in molecular DMRG calculations will be implemented and applied. In addition, our code will be supplemented by a novel

automated selection scheme for large-scale active spaces as well as the ability to calculate nonadiabatic coupling coefficients to study chemical reactions on multiple adiabatic surfaces.

Publications resulting from this research area: 136, 138

External funding: none

Cooperations: G. K.-L. Chan (Princeton, NJ, US), V. Krewald (Wien, AT), D. Pantazis (Mülheim, DE), S. Sharma (Boulder, CO, US)

2.5.9 Publications 2014-2016 from the Department of Theory

Thiel group

(1) Altun, A.; Breidung, J.; Neese, F.; Thiel, W. *J. Chem. Theory Comput.* **2014**, *10*, 3807-3820.

(2) Boulanger, E.; Thiel, W. *J. Chem. Theory Comput.* **2014**, *10*, 1795-1809.

(3) Cui, G.; Thiel, W. *J. Phys. Chem. Lett.* **2014**, *5*, 2682-2687.

(4) Cui, G.; Thiel, W. *J. Chem. Phys.* **2014**, *141*, 124101 / 1-13.

(5) Escudero, D.; Thiel, W. *J. Chem. Phys.* **2014**, *140*, 194105 / 1-8.

(6) Escudero, D.; Thiel, W. *Inorg. Chem.* **2014**, *53*, 11015-11019.

(7) Gámez, J. A.; Koslowski, A.; Thiel, W. *RSC Adv.* **2014**, *4*, 1886-1889.

(8) Götze, J. P.; Kröner, D.; Banerjee, S.; Karasulu, B.; Thiel, W. *ChemPhysChem* **2014**, *15*, 3392-3401.

(9) Gu, L.; Gopakumar, G.; Gualco, P.; Thiel, W.; Alcarazo, M. *Chem.– Eur. J.* **2014**, *20*, 8575-8578.

(10) Karasulu, B.; Götze, J. P.; Thiel, W. *J. Chem. Theory Comput.* **2014**, *10*, 5549-5566.

(11) Loerbroks, C.; Böker, B.; Cordes, J.; Barrett, A. G. M.; Thiel, W. *Eur. J. Org. Chem.* **2014**, 5476-5486.

(12) Loerbroks, C.; van Rijn, J.; Ruby, M.-P.; Tong, Q.; Schüth, F.; Thiel, W. *Chem.– Eur. J.* **2014**, *20*, 12298-12309.

(13) Luzio, A.; Fazzi, D.; Nübling, F.; Matsidik, R.; Straub, A.; Komber, H.; Giussani, E.; Watkins, S. E.; Barbatti, M.; Thiel, W.; Gann, E.; Thomsen, L.; McNeill, C. R.; Caironi, M.; Sommer, M. *Chem. Mater.* **2014**, *26*, 6233-6240.

(14) Marian, C. M.; Nakagawa, S.; Rai-Constapel, V.; Karasulu, B.; Thiel, W. *J. Phys. Chem. B* **2014**, *118*, 1743-1753.

(15) Nikiforov, A.; Gamez, J. A.; Thiel, W.; Huix-Rotllant, M.; Filatov, M. *J. Chem. Phys.* **2014**, *141*, 124122 / 1-16.

(16) Saito, T.; Thiel, W. *J. Phys. Chem. B* **2014**, *118*, 5034-5043.

(17) Seidel, G.; Gabor, B.; Goddard, R.; Heggen, B.; Thiel, W.; Fürstner, A. *Angew. Chem., Int. Ed.* **2014**, *53*, 879-882.

(18) Sen, K.; Thiel, W. *J. Phys. Chem. B* **2014**, *118*, 2810-2820.

(19) Sen, K.; Crespo-Otero, R.; Thiel, W.; Barbatti, M. *Comput. Theor. Chem.* **2014**, *1040–1041*, 237-242.

(20) Shaik, S.; Chen, H.; Usharani, D.; Thiel, W. In *Drug Metabolism Prediction*; Kirchmair, J., Ed.; Wiley-VCH: Weinheim, 2014; pp 133-177.

(21) Spörkel, L.; Cui, G.; Koslowski, A.; Thiel, W. *J. Phys. Chem. A* **2014**, *118*, 152-157.
(22) Thiel, W. *WIREs Comput. Mol. Sci.* **2014**, *4*, 145-157.
(23) Thiel, W. *Angew. Chem., Int. Ed.* **2014**, *53*, 8605-8613.
(24) Wolf, L. M.; Thiel, W. *J. Org. Chem.* **2014**, *79*, 12136-12147.
(25) Zhang, Q.; Chen, X.; Cui, G.; Fang, W.-H.; Thiel, W. *Angew. Chem., Int. Ed.* **2014**, *53*, 8649-8653.
(26) Buchner, F.; Heggen, B.; Ritze, H.-H.; Thiel, W.; Lübcke, A. *Phys. Chem. Chem. Phys.* **2015**, *17*, 31978-31987.
(27) Ceausu-Velcescu, A.; Pracna, P.; Breidung, J.; Thiel, W.; Badaoui, M. *J. Mol. Spectrosc.* **2015**, *316*, 11-21.
(28) Chang, X.-P.; Cui, G.; Fang, W.-H.; Thiel, W. *ChemPhysChem* **2015**, *16*, 933-937.
(29) Dral, P. O.; von Lilienfeld, O. A.; Thiel, W. *J. Chem. Theory Comput.* **2015**, *11*, 2120-2125.
(30) Escudero, D.; Thiel, W.; Champagne, B. *Phys. Chem. Chem. Phys.* **2015**, *17*, 18908-18912.
(31) Fazzi, D.; Barbatti, M.; Thiel, W. *Phys. Chem. Chem. Phys.* **2015**, *17*, 7787-7799.
(32) Götze, J. P.; Karasulu, B.; Patil, M.; Thiel, W. *Biochim. Biophys. Acta, Bioenerg.* **2015**, *1847*, 1509-1517.
(33) Holle, S.; Escudero, D.; Inés, B.; Rust, J.; Thiel, W.; Alcarazo, M. *Chem.– Eur. J.* **2015**, *21*, 2744-2749.
(34) Ilg, M. K.; Wolf, L. M.; Mantilli, L.; Farès, C.; Thiel, W.; Fürstner, A. *Chem.– Eur. J.* **2015**, *21*, 12279-12284.
(35) Karasulu, B.; Thiel, W. *J. Phys. Chem. B* **2015**, *119*, 928-943.
(36) Karasulu, B.; Thiel, W. *ACS Catal.* **2015**, *5*, 1227-1239.
(37) Leutzsch, M.; Wolf, L. M.; Gupta, P.; Fuchs, M.; Thiel, W.; Farès, C.; Fürstner, A. *Angew. Chem., Int. Ed.* **2015**, *54*, 12431-12436.
(38) Liu, L.; Leutzsch, M.; Zheng, Y.; Alachraf, M. W.; Thiel, W.; List, B. *J. Am. Chem. Soc.* **2015**, *137*, 13268-13271.
(39) Loerbroks, C.; Boulanger, E.; Thiel, W. *Chem.– Eur. J.* **2015**, *21*, 5477-5487.
(40) Loerbroks, C.; Heimermann, A.; Thiel, W. *J. Comput. Chem.* **2015**, *36*, 1114-1123.
(41) Lu, Y.; Lan, Z.; Thiel, W. In *Photoinduced Phenomena in Nucleic Acids II*; Barbatti, M., Borin, A. C., Ullrich, S., Eds.; *Topics in Current Chemistry*; Springer: Berlin, 2015; Vol. 356; pp 89-122.

(42) Mancini, D. T.; Sen, K.; Barbatti, M.; Thiel, W.; Ramalho, T. C. *ChemPhysChem* **2015**, *16*, 3444-3449.

(43) Owens, A.; Yurchenko, S. N.; Yachmenev, A.; Tennyson, J.; Thiel, W. *J. Chem. Phys.* **2015**, *142*, 244306 / 1-10.

(44) Owens, A.; Yurchenko, S. N.; Thiel, W.; Špirko, V. *Mon. Not. R. Astron. Soc.* **2015**, *450*, 3191-3200.

(45) Owens, A.; Yurchenko, S. N.; Polyansky, O. L.; Ovsyannikov, R. I.; Thiel, W.; Špirko, V. *Mon. Not. R. Astron. Soc.* **2015**, *454*, 2292-2298.

(46) Owens, A.; Yurchenko, S. N.; Yachmenev, A.; Thiel, W. *J. Chem. Phys.* **2015**, *143*, 244317 / 1-12.

(47) Sauer, S. P. A.; Pitzner-Frydendahl, H. F.; Buse, M.; Jensen, H. J. A.; Thiel, W. *Mol. Phys.* **2015**, *113*, 2026-2045.

(48) Schwab, M. G.; Takase, M.; Mavrinsky, A.; Pisula, W.; Feng, X.; Gámez, J. A.; Thiel, W.; Mali, K. S.; de Feyter, S.; Müllen, K. *Chem.– Eur. J.* **2015**, *21*, 8426-8434.

(49) Sokkar, P.; Boulanger, E.; Thiel, W.; Sanchez-Garcia, E. *J. Chem. Theory Comput.* **2015**, *11*, 1809-1818.

(50) Spörkel, L.; Jankowska, J.; Thiel, W. *J. Phys. Chem. B* **2015**, *119*, 2702-2710.

(51) Vasilevskaya, T.; Khrenova, M. G.; Nemukhin, A. V.; Thiel, W. *J. Comput. Chem.* **2015**, *36*, 1621-1630.

(52) Willwacher, J.; Heggen, B.; Wirtz, C.; Thiel, W.; Fürstner, A. *Chem.–Eur. J.* **2015**, *21*, 10416-10430.

(53) Xia, S.-H.; Xie, B.-B.; Fang, Q.; Cui, G.; Thiel, W. *Phys. Chem. Chem. Phys.* **2015**, *17*, 9687-9697.

(54) Xie, L.-G.; Bagutski, V.; Audisio, D.; Wolf, L. M.; Schmidts, V.; Hofmann, K.; Wirtz, C.; Thiel, W.; Thiele, C. M.; Maulide, N. *Chem. Sci.* **2015**, *6*, 5734-5739.

(55) Boess, E.; Wolf, L. M.; Malakar, S.; Salamone, M.; Bietti, M.; Thiel, W.; Klussmann, M. *ACS Catal.* **2016**, *6*, 3253-3261.

(56) Chang, X.-P.; Zheng, Y.; Cui, G.; Fang, W.-H.; Thiel, W. *Phys. Chem. Chem. Phys.* **2016**, *18*, 24713-24721.

(57) Das, S.; Liu, L.; Zheng, Y.; Alachraf, M. W.; Thiel, W.; De, C. K.; List, B. *J. Am. Chem. Soc.* **2016**, *138*, 9429-9432.

(58) Dral, P. O.; Wu, X.; Spörkel, L.; Koslowski, A.; Weber, W.; Steiger, R.; Scholten, M.; Thiel, W. *J. Chem. Theory Comput.* **2016**, *12*, 1082-1096.

(59) Dral, P. O.; Wu, X.; Spörkel, L.; Koslowski, A.; Thiel, W. *J. Chem. Theory Comput.* **2016**, *12*, 1097-1120.

(60) Dube, J. W.; Zheng, Y.; Thiel, W.; Alcarazo, M. *J. Am. Chem. Soc.* **2016**, *138*, 6869-6877.

(61) Escorcia, A. M.; Sen, K.; Daza, M. C.; Doerr, M.; Thiel, W. *ACS Catal*. **2016**, DOI: 10.1021/acscatal.6b02310.

(62) Fazzi, D.; Barbatti, M.; Thiel, W. *J. Am. Chem. Soc.* **2016**, *138*, 4502-4511.

(63) Ganguly, A.; Manahan, C. C.; Top, D.; Yee, E. F.; Lin, C.; Young, M. W.; Thiel, W.; Crane, B. R. *Proc. Natl. Acad. Sci. U.S.A.* **2016**, *113*, 10073-10078.

(64) Guo, Y.; Beyle, F. E.; Bold, B. M.; Watanabe, H. C.; Koslowski, A.; Thiel, W.; Hegemann, P.; Marazzi, M.; Elstner, M. *Chem. Sci.* **2016**, *7*, 3879-3891.

(65) Heggen, B.; Patil, M.; Thiel, W. *J. Comput. Chem.* **2016**, *37*, 280-285.

(66) Heggen, B.; Thiel, W. *J. Organomet. Chem.* **2016**, *804*, 42-47.

(67) Henkel, S.; Costa, P.; Klute, L.; Sokkar, P.; Fernandez-Oliva, M.; Thiel, W.; Sanchez-Garcia, E.; Sander, W. *J. Am. Chem. Soc.* **2016**, *138*, 1689-1697.

(68) Huix-Rotllant, M.; Nikiforov, A.; Thiel, W.; Filatov, M. In *Density-Functional Methods for Excited States*; Ferré, N., Filatov, M., Huix-Rotllant, M., Eds.; *Topics in Current Chemistry*; Springer International Publishing: Berlin, 2016; Vol. 368; pp 445-476.

(69) Kahmann, S.; Fazzi, D.; Matt, G. J.; Thiel, W.; Loi, M. A.; Brabec, C. J. *J. Phys. Chem. Lett.* **2016**, *7*, 4438-4444.

(70) Knorr, J.; Sokkar, P.; Schott, S.; Costa, P.; Thiel, W.; Sander, W.; Sanchez-Garcia, E.; Nuernberger, P. *Nat. Commun.* **2016**, *7*, 12968.

(71) König, G.; Pickard, F. C.; Huang, J.; Simmonett, A. C.; Tofoleanu, F.; Lee, J.; Dral, P. O.; Prasad, S.; Jones, M.; Shao, Y.; Thiel, W.; Brooks, B. R. *J. Comput. Aided Mol. Des.* **2016**, DOI: 10.1007/s10822-016-9936-x.

(72) Kötzner, L.; Leutzsch, M.; Sievers, S.; Patil, S.; Waldmann, H.; Zheng, Y.; Thiel, W.; List, B. *Angew. Chem., Int. Ed.* **2016**, *55*, 7693-7697.

(73) Liu, X.-Y.; Chang, X.-P.; Xia, S.-H.; Cui, G.; Thiel, W. *J. Chem. Theory Comput.* **2016**, *12*, 753-764.

(74) Lombeck, F.; Komber, H.; Fazzi, D.; Nava, D.; Kuhlmann, J.; Stegerer, D.; Strassel, K.; Brandt, J.; de Zerio Mendaza, A. D.; Müller, C.; Thiel, W.; Caironi, M.; Friend, R.; Sommer, M.; *Adv. Energy Mat.* **2016**, *6*, 1601232.

(75) Monaco, M. R.; Fazzi, D.; Tsuji, N.; Leutzsch, M.; Liao, S.; Thiel, W.; List, B. *J. Am. Chem. Soc.* **2016**, *138*, 14740-14749.

(76) Nikiforov, A.; Gamez, J. A.; Thiel, W.; Filatov, M. *J. Phys. Chem. Lett.* **2016**, *7*, 105-110.

(77) Owens, A.; Yurchenko, S. N.; Thiel, W.; Špirko, V. *Phys. Rev. A* **2016**, *93*, 052506.

(78) Owens, A.; Yurchenko, S. N.; Yachmenev, A.; Tennyson, J.; Thiel, W. *J. Quant. Spectrosc. Radiat. Transfer* **2016**, *184*, 100-110.
(79) Owens, A.; Yurchenko, S. N.; Yachmenev, A.; Tennyson, J.; Thiel, W. *J. Chem. Phys.* **2016**, *145*, 104305 / 1-13.
(80) Patil, M.; Thiel, W. *Eur. J. Org. Chem.* **2016**, 830-839.
(81) Spörkel, L.; Thiel, W. *J. Chem. Phys.* **2016**, *144*, 194108 / 1-8.
(82) Tuna, D.; Lu, Y.; Koslowski, A.; Thiel, W. *J. Chem. Theory Comput.* **2016**, *12*, 4400-4422.
(83) Vasilevskaya, T.; Khrenova, M. G.; Nemukhin, A. V.; Thiel, W. *J. Comput. Chem.* **2016**, *37*, 1801-1809.
(84) Vasilevskaya, T.; Khrenova, M. G.; Nemukhin, A. V.; Thiel, W. *Mendeleev Commun.* **2016**, *26*, 209-211.
(85) Vasilevskaya, T.; Thiel, W. *J. Chem. Theory Comput.* **2016**, *12*, 3561-3570.
(86) Wang, S.; Sun, H.; Ail, U.; Vagin, M.; Persson, P. O. Å.; Andreasen, J. W.; Thiel, W.; Berggren, M.; Crispin, X.; Fazzi, D.; Fabiano, S. *Adv. Mater.* **2016**, DOI: 10.1002/adma.201603731.
(87) Wang, Y.-T.; Liu, X.-Y.; Cui, G.; Fang, W.-H.; Thiel, W. *Angew. Chem., Int. Ed.* **2016**, *55*, 14009-14013.
(88) Wu, X.; Koslowski, A.; Thiel, W. In *Electronic Structure Calculations on Graphics Processing Units: From Quantum Chemistry to Condensed Matter Physics*; Walker, R. C., Goetz, A. W., Eds.; John Wiley & Sons: Chichester, 2016; pp 239-257.
(89) Xia, S.-H.; Cui, G.; Fang, W.-H.; Thiel, W. *Angew. Chem., Int. Ed.* **2016**, *55*, 2067-2072.
(90) Xie, Y.; Cheng, G.-J.; Thiel, W.; List, B. *J. Am. Chem. Soc.* **2016**, *138*, 14538-14541.

Barbatti group

(13) Luzio, A.; Fazzi, D.; Nübling, F.; Matsidik, R.; Straub, A.; Komber, H.; Giussani, E.; Watkins, S. E.; Barbatti, M.; Thiel, W.; Gann, E.; Thomsen, L.; McNeill, C. R.; Caironi, M.; Sommer, M. *Chem. Mater.* **2014**, *26*, 6233-6240.
(19) Sen, K.; Crespo-Otero, R.; Thiel, W.; Barbatti, M. *Comput. Theor. Chem.* **2014**, *1040–1041*, 237-242.
(31) Fazzi, D.; Barbatti, M.; Thiel, W. *Phys. Chem. Chem. Phys.* **2015**, *17*, 7787-7799.

(42) Mancini, D. T.; Sen, K.; Barbatti, M.; Thiel, W.; Ramalho, T. C. *ChemPhysChem* **2015**, *16*, 3444-3449.
(62) Fazzi, D.; Barbatti, M.; Thiel, W. *J. Am. Chem. Soc.* **2016**, *138*, 4502-4511.
(91) Antol, I.; Glasovac, Z.; Crespo-Otero, R.; Barbatti, M. *J. Chem. Phys.* **2014**, *141*, 074307.
(92) Barbatti, M.; Ruckenbauer, M.; Plasser, F.; Pittner, J.; Granucci, G.; Persico, M.; Lischka, H. *WIREs Comput. Mol. Sci.* **2014**, *4*, 26-33.
(93) Barbatti, M. *J. Am. Chem. Soc.* **2014**, *136*, 10246-10249.
(94) Barbatti, M. *ChemPhysChem* **2014**, *15*, 3342-3354.
(95) Crespo-Otero, R.; Mardykov, A.; Sanchez-Garcia, E.; Sander, W.; Barbatti, M. *Phys. Chem. Chem. Phys.* **2014**, *16*, 18877-18887.
(96) Kungwan, N.; Kerdpol, K.; Daengngern, R.; Hannongbua, S.; Barbatti, M. *Theor. Chem. Acc.* **2014**, *133*, 1-11.
(97) Pereira Rodrigues, G.; Ventura, E.; do Monte, S. A.; Barbatti, M. *J. Phys. Chem. A* **2014**, *118*, 12041-12049.
(98) Plasser, F.; Crespo-Otero, R.; Pederzoli, M.; Pittner, J.; Lischka, H.; Barbatti, M. *J. Chem. Theory Comput.* **2014**, *10*, 1395-1405.
(99) West, A. C.; Barbatti, M.; Lischka, H.; Windus, T. L. *Comput. Theor. Chem.* **2014**, *1040–1041*, 158-166.
(100) Barbatti, M.; Lischka, H. *Phys. Chem. Chem. Phys.* **2015**, *17*, 15452-15459.
(101) Barbatti, M.; Borin, A. C.; Ullrich, S. In *Photoinduced Phenomena in Nucleic Acids I*; Barbatti, M., Borin, A. C., Ullrich, S., Eds.; *Top. Curr. Chem.*; Springer: Berlin, 2015; Vol. 355; pp 1-32.
(102) Cardozo, T. M.; Aquino, A. J. A.; Barbatti, M.; Borges, I.; Lischka, H. *J. Phys. Chem. A* **2015**, *119*, 1787-1795.
(103) Crespo-Otero, R.; Kungwan, N.; Barbatti, M. *Chem. Sci.* **2015**, *6*, 5762-5767.
(104) Stojanović, L.; Rodrigues, G. P.; Aziz, S. G.; Hilal, R. H.; Barbatti, M. *RSC Adv.* **2015**, *5*, 97003-97015.
(105) Arbelo-González, W.; Crespo-Otero, R.; Barbatti, M. *J. Chem. Theory Comput.* **2016**, *12*, 5037-5049.
(106) Barbatti, M.; Crespo-Otero, R. In *Density-Functional Methods for Excited States*; Ferré, N., Filatov, M., Huix-Rotllant, M., Eds.; Springer International Publishing: Cham, 2016; pp 415-444.
(107) Pereira Rodrigues, G.; Ventura, E.; Andrade do Monte, S.; Barbatti, M. *J. Comput. Chem.* **2016**, *37*, 675-683.

Sánchez-García group

(49) Sokkar, P.; Boulanger, E.; Thiel, W.; Sanchez-Garcia, E. *J. Chem. Theory Comput.* **2015**, *11*, 1809-1818.

(67) Henkel, S.; Costa, P.; Klute, L.; Sokkar, P.; Fernandez-Oliva, M.; Thiel, W.; Sanchez-Garcia, E.; Sander, W. *J. Am. Chem. Soc.* **2016**, *138*, 1689-1697.

(70) Knorr, J.; Sokkar, P.; Schott, S.; Costa, P.; Thiel, W.; Sander, W.; Sanchez-Garcia, E.; Nuernberger, P. *Nat. Commun.* **2016**, *7*, 12968.

(95) Crespo-Otero, R.; Mardykov, A.; Sanchez-Garcia, E.; Sander, W.; Barbatti, M. *Phys. Chem. Chem. Phys.* **2014**, *16*, 18877-18887.

(108) Bravo-Rodriguez, K.; Ismail-Ali, A. F.; Klopries, S.; Kushnir, S.; Ismail, S.; Fansa, E. K.; Wittinghofer, A.; Schulz, F.; Sanchez-Garcia, E. *ChemBioChem* **2014**, *15*, 1991-1997.

(109) Costa, P.; Fernandez-Oliva, M.; Sanchez-Garcia, E.; Sander, W. *J. Am. Chem. Soc.* **2014**, *136*, 15625-15630.

(110) Klopries, S.; Koopmans, K. R. M.; Sanchez-Garcia, E.; Schulz, F. *ChemBioChem* **2014**, *15*, 495-497.

(111) Merten, C.; Li, F.; Bravo-Rodriguez, K.; Sanchez-Garcia, E.; Xu, Y.; Sander, W. *Phys. Chem. Chem. Phys.* **2014**, *16*, 5627-5633.

(112) Sander, W.; Roy, S.; Bravo-Rodriguez, K.; Grote, D.; Sanchez-Garcia, E. *Chem.–Eur. J.* **2014**, *20*, 12917-12923.

(113) Bravo-Rodriguez, K.; Klopries, S.; Koopmans, Kyra R. M.; Sundermann, U.; Yahiaoui, S.; Arens, J.; Kushnir, S.; Schulz, F.; Sanchez-Garcia, E. *Chem. Biol. (Oxford, U. K.)* **2015**, *22*, 1425-1430.

(114) Costa, P.; Trosien, I.; Fernandez-Oliva, M.; Sanchez-Garcia, E.; Sander, W. *Angew. Chem., Int. Ed.* **2015**, *54*, 2656-2660.

(115) Hanke, K.; Kaufmann, M.; Schwaab, G.; Havenith, M.; Wolke, C. T.; Gorlova, O.; Johnson, M. A.; Kar, B. P.; Sander, W.; Sanchez-Garcia, E. *Phys. Chem. Chem. Phys.* **2015**, *17*, 8518-8529.

(116) Klopries, S.; Bravo-Rodriguez, K.; Koopmans, K. R. M.; Sundermann, U.; Yahiaoui, S.; Arens, J.; Kushnir, S.; Sanchez-Garcia, E.; Schulz, F. *Data in Brief* **2015**, *5*, 528-536.

(117) Lopes, D. H. J.; Attar, A.; Nair, G.; Hayden, E. Y.; Du, Z.; McDaniel, K.; Dutt, S.; Bandmann, H.; Bravo-Rodriguez, K.; Mittal, S.; Klärner, F.-G.; Wang, C.; Sanchez-Garcia, E.; Schrader, T.; Bitan, G. *ACS Chem. Biol.* **2015**, *10*, 1555-1569.

(118) Lump, E. et al.; Kelly, J. W., Ed.; eLife Sciences Publications, Ltd: Cambridge, UK, **2015**, p 4:e05397.
(119) Martinez Gonzalez, M.; Bravo-Rodriguez, K.; Suardiaz, R.; Garcia de la Vega, J. M.; Montero, L. A.; Sanchez-Garcia, E.; Crespo-Otero, R. *Theor. Chem. Acc.* **2015**, *134*, 88 / 1-12.
(120) Arumughan, A.; Roske, Y.; Barth, C.; Forero, L.; Bravo-Rodriguez, K.; Redel , A.; Faelber, K.; Rau, K.; Mielke, T.; Daumke, O.; Sanchez-Garcia, E.; Rocks, O.; Panakova, D.; Heinemann, U.; Wanker, E. *Nat. Commun.* **2016**, *7*, 13047.
(121) Bettinger, H. F.; Tönshoff, C.; Doerr, M.; Sanchez-Garcia, E. *J. Chem. Theory Comput.* **2016**, *12*, 305-312.
(122) Costa, P.; Lohmiller, T.; Trosien, I.; Savitsky, A.; Lubitz, W.; Fernandez-Oliva, M.; Sanchez-Garcia, E.; Sander, W. *J. Am. Chem. Soc.* **2016**, *138*, 1622-1629.
(123) Trusch, F.; Kowski, K.; Bravo-Rodriguez, K.; Beuck, C.; Sowislok, A.; Wettig, B.; Matena, A.; Sanchez-Garcia, E.; Meyer, H.; Schrader, T.; Bayer, P. *Chem. Commun.* **2016**, DOI: 10.1039/c6cc08039a.

Heyden group

(124) Heyden, M.; Schwaab, G.; Havenith, M. *J. Phys. Chem. B* **2014**, *118*, 10802-10805.
(125) Heyden, M. *J. Chem. Phys.* **2014**, *141*, 22D509 / 1-10.
(126) Heyden, M. *GIT Labor-Fachzeitschrift* **2014**, 48-51.
(127) Capponi, S.; Heyden, M.; Bondar, A.-N.; Tobias, D. J.; White, S. H. *Proc. Natl. Acad. Sci. U.S.A.* **2015**, *112*, 9016-9021.
(128) Fichou, Y.; Heyden, M.; Zaccai, G.; Weik, M.; Tobias, D. J. *J. Phys. Chem. B* **2015**, *119*, 12580-12589.
(129) Gnutt, D.; Gao, M.; Brylski, O.; Heyden, M.; Ebbinghaus, S. *Angew. Chem., Int. Ed.* **2015**, *54*, 2548-2551.
(130) Heyden, M. In *Computational Trends in Solvation and Transport in Liquids*; Sutmann, G., Grotendorst, J., Gompper, G., Marx, D., Eds.; *Schriften des Forschungszentrums Jülich - IAS Series*; Forschungszentrum Jülich GmbH: Jülich, 2015; Vol. 28; pp 129-147.
(131) Prytkova, V.; Heyden, M.; Tobias, D.; Freites, J. A. *Biophys. J.* **2015**, *108*, 470a.
(132) Schirò, G.; Fichou, Y.; Gallat, F.-X.; Wood, K.; Gabel, F.; Moulin, M.; Härtlein, M.; Heyden, M.; Colletier, J.-P.; Orecchini, A.; Paciaroni, A.; Wuttke, J.; Tobias, D. J.; Weik, M. *Nat. Commun.* **2015**, *6*, 6490.
(133) Weiß, R. G.; Heyden, M.; Dzubiella, J. *Phys. Rev. Lett.* **2015**, *114*, 187802.

(134) Fisette, O.; Päslack, C.; Barnes, R.; Isas, J. M.; Langen, R.; Heyden, M.; Han, S.; Schäfer, L. V. *J. Am. Chem. Soc.* **2016**, *138*, 11526-11535.
(135) Gnutt, D.; Ebbinghaus, S.; Heyden, M. *Nachr. Chem.* **2016**, *64*, 310-313.

Roemelt group

(136) Roemelt, M. *J. Chem. Phys.* **2015**, *143*, 044112.
(137) Vliegenthart, A. B.; Welling, F. A. L.; Roemelt, M.; Klein Gebbink, R. J. M.; Otte, M. *Org. Lett.* **2015**, *17*, 4172-4175.
(138) Roemelt, M.; Guo, S.; Chan, G. K.-L. *J. Chem. Phys.* **2016**, *144*, 204113 / 1-12.

Publications by Other Members of the Department

(139) Bellani, S.; **Fazzi**, D.; Bruno, P.; Giussani, E.; Canesi, E. V.; Lanzani, G.; Antognazza, M. R. *J. Phys. Chem. C* **2014**, *118*, 6291-6299.
(140) Caddeo, C.; **Fazzi**, D.; Caironi, M.; Mattoni, A. *J. Phys. Chem. B* **2014**, *118*, 12556-12565.
(141) D'Innocenzo, V.; Luzio, A.; Petrozza, A.; **Fazzi**, D.; Caironi, M. *Adv. Funct. Mater.* **2014**, *24*, 5584-5593.
(142) **Escudero**, D.; Frontera, A.; Streubel, R. *ChemPhysChem* **2014**, *15*, 1599-1603.
(143) Idé, J.; **Fazzi**, D.; Casalegno, M.; Meille, S. V.; Raos, G. *Journal of Materials Chemistry C* **2014**, *2*, 7313-7325.
(144) Martino, N.; **Fazzi,** D.; Sciascia, C.; Luzio, A.; Antognazza, M. R.; Caironi, M. *ACS Nano* **2014**, *8*, 5968-5978.
(145) Ramakrishnan, R.; **Dral**, P. O.; Rupp, M.; von Lilienfeld, O. A. *Sci. Data* **2014**, *1*, 140022.
(146) Seidel, R. W.; Goddard, R.; **Breidung**, J.; Jäger, E.-G. *Z. Anorg. Allg. Chem.* **2014**, *640*, 1946-1952.
(147) Singh, R.; Giussani, E.; Mróz, M. M.; Di Fonzo, F.; **Fazzi**, D.; Cabanillas-González, J.; Oldridge, L.; Vaenas, N.; Kontos, A. G.; Falaras, P.; Grimsdale, A. C.; Jacob, J.; Müllen, K.; Keivanidis, P. E. *Org. Electron.* **2014**, *15*, 1347-1361.
(148) Tommasini, M.; Milani, A.; **Fazzi**, D.; Lucotti, A.; Castiglioni, C.; Januszewski, J. A.; Wendinger, D.; Tykwinski, R. R. *J. Phys. Chem. C* **2014**, *118*, 26415-26425.
(149) **Arbelo-González**, W.; Bonnet, L.; García-Vela, A. *J. Chem. Phys.* **2015**, *142*, 134111.
(150) **Fazzi**, D.; Caironi, M. *Phys. Chem. Chem. Phys.* **2015**, *17*, 8573-8590.

(151) Giussani, E.; Brambilla, L.; **Fazzi**, D.; Sommer, M.; Kayunkid, N.; Brinkmann, M.; Castiglioni, C. *J. Phys. Chem. B* **2015**, *119*, 2062-2073.

(152) Matsidik, R.; Martin, J.; Schmidt, S.; Obermayer, J.; Lombeck, F.; Nübling, F.; Komber, H.; **Fazzi**, D.; Sommer, M. *J. Org. Chem.* **2015**, *80*, 980-987.

(153) Muya, J. T.; Ceulemans, A.; **Gopakumar**, G.; Parish, C. A. *J. Phys. Chem. A* **2015**, *119*, 4237-4243.

(154) Ramakrishnan, R.; **Dral**, P. O.; Rupp, M.; von Lilienfeld, O. A. *J. Chem. Theory Comput.* **2015**, *11*, 2087-2096.

(155) Trujillo, C.; **Gámez**, J. A. *Comput. Theor. Chem.* **2015**, *1052*, 68-72.

(156) **Tuna**, D.; Lefrancois, D.; Wolański, Ł.; Gozem, S.; Schapiro, I.; Andruniów, T.; Dreuw, A.; Olivucci, M. *J. Chem. Theory Comput.* **2015**, *11*, 5758-5781.

(157) Maciejewski, J.; Sobczuk, A.; Claveau, A.; Nicolai, A.; Petraglia, R.; Cervini, L.; Baudat, E.; Mieville, P.; **Fazzi**, D.; Corminboeuf, C.; Sforazzini, G. *Chem. Sci.* **2016**, DOI: 10.1039/C6SC03196J.

(158) Meinhardt, U.; Lodermeyer, F.; Schaub, T. A.; Kunzmann, A.; **Dral**, P. O.; Sale, A. C.; Hampel, F.; Guldi, D. M.; Costa, R. D.; Kivala, M. *RSC Adv.* **2016**, *6*, 67372-67377.

(159) Pickard, F. C.; **König**, G.; Simmonett, A. C.; Shao, Y.; Brooks, B. R. *Bioorg. Med. Chem.* **2016**, *24*, 4988-4997.

(160) Pickard, F. C.; **König**, G.; Tofoleanu, F.; Lee, J.; Simmonett, A. C.; Shao, Y.; Ponder, J. W.; Brooks, B. R. *J. Comput. Aided Mol. Des.* **2016**, DOI 10.1007/s10822-016-9955-7.

(161) Tofoleanu, F.; Lee, J.; Pickard, F. C.; **König**, G.; Huang, J.; Baek, M.; Seok, C.; Brooks, B. R. *J. Comput.-Aided Mol. Des.* **2016**, DOI: 10.1007/s10822-016-9965-5.

(162) **Tuna**, D.; Domcke, W. *Phys. Chem. Chem. Phys.* **2016**, *18*, 947-955.

(163) **Tuna**, D.; Sobolewski, A. L.; Domcke, W. *J. Phys. Chem. B* **2016**, *120*, 10729-10735.

(164) Yin, J.; Wang, Z.; **Fazzi**, D.; Shen, Z.; Soci, C. *J. Phys. Chem. C* **2016**, *120*, 1994-2001.

Publications by other members of the Department (marked in bold) are included only if they carry the address of the Institute.

There are nine joint theory papers, which are listed twice but with a unique number. Joint research projects between the Thiel group and experimental groups in the Institute are documented in fifteen joint publications, which are listed both here and in the section of the experimental partner.